Geological Quarterly, 2010, **54** (3): 301–324

Variscan multistage granitoid magmatism in Brunovistulicum: petrological and SHRIMP U-Pb zircon geochronological evidence from the southern part of the Strzelin Massif, SW Poland

Teresa OBERC-DZIEDZIC, Ryszard KRYZA and Joanna BIAŁEK

Oberc-Dziedzic T., Kryza R. and Białek J. (2010) – Variscan multistage granitoid magmatism in Brunovistulicum: petrological and SHRIMP U-Pb zircon geochronological evidence from the southern part of the Strzelin Massif, SW Poland. Geol. Quart., **54** (3): 301–324. Warszawa.

U-Pb SHRIMP ages of one granodiorite and two tonalite samples from the Strzelin Massif, northern part of Brunovistulicum, reveal three distinct stages of Carboniferrous–early Permian granitoid magmatism: tonalitic I − 324 Ma, granodioritic – 305 Ma and tonalitic II/granitic – 295 Ma. The first stage of magmatism coincided with the first migmatization event which took place shortly after the first deformation. The second stage of granitoid plutonism was coeval with the second migmatization event which produced abundant pegmatites. It took place after compressional phases of the second deformation and was related to decompression at the beginning of tectonic denudation. The third, most abundant stage of magmatism was connected with late extension in that part of the Variscan Orogen.

Teresa Oberc-Dziedzic, Ryszard Kryza and Joanna Białek, Institute of Geological Sciences, University of Wrocław, Plac M. Borna 9, PL-50-204 Wrocław, Poland, e-mail: teresa.oberc-dziedzic@ing.uni.wroc.pl (received: June 24, 2010; accepted: October 12, 2010).

Key words: Variscides, Bohemian Massif, Strzelin Massif, zircon SHRIMP geochronology, granitoids.

INTRODUCTION

The Bohemian Massif, near the eastern termination of the European Variscan belt, is subdivided into the Moldanubian, Saxothuringian (Kossmat, 1927) and Teplá-Barrandian (Franke, 1989) tectono-stratigraphic zones, interpreted by some authors as terranes (Matte *et al*., 1990) of the Armorican Terrane Assemblage (Franke, 2000). The location, extent and correlations of these zones in the Sudetes is still a matter of discussion (e.g., Franke *et al*., 1993; Cymerman and Piasecki, 1994; Cymerman *et al*., 1997; Franke and Żelaźniewicz, 2000, 2002; Aleksandrowski and Mazur, 2002). Along the eastern margin of the Bohemian Massif, the Moldanubian Zone adjoins Brunovistulicum (Brunia after Zapletal, 1933, *fide*: Dudek, 1980; Bruno-Vistulicum after Dudek, 1980; the Brunia continent, Schulmann *et al*., 2009; Brunovistulia, Żelaźniewicz *et al*., 2009) of the Avalonian affinity (Finger *et al*., 2000; Friedl *et al*., 2000). The boundary between these was recognized by Suess (1912, 1926) as the Moldanubian Overthrust. The Nyznerov Thrust (Skácel, 1989) in the East Sudetes and the Strzelin Thrust in the Fore-Sudetic Block (Oberc-Dziedzic *et al*., 2005; Żelaźniewicz and Aleksandrowski, 2008; Fig. 1) are regarded as the NE continuation of the Moldanubian Overthrust. During the early Carboniferous oblique collision of the Moldanubian and Brunovistulian terranes (Schulmann and Gayer, 2000), the marginal part of Brunovistulicum, composed of Neoproterozoic granites, together with their sedimentary cover, was deformed into the nappe piles of the Moravo-Silesian Zone (e.g., Finger *et al*., 1989; Franke and Żelaźniewicz, 2000; Mazur *et al*., 2006). The rocks of the Moravo-Silesian Zone emerge through the Moldanubian rocks in the southern Thaya Window, the central Svratka Window and the northern Silesian domain (e.g., Schulmann and Gayer, 2000), named Silesicum by Suess (1912), which comprises the Velké Vbrno and Keprník nappes as well as parautochthonous gneisses of the Desna Dome and their volcano-sedimentary Devonian cover of the Vrbno Group (Cháb *et al*., 1984; Mazur *et al*., 2006). The northern continuation of Brunovistulicum was identified in the Strzelin Massif, in the Fore-Sudetic Block (Oberc-Dziedzic *et al*., 2003*a*; Żelaźniewicz and Aleksandrowski, 2008; Fig. 2), as represented by Neoproterozoic gneisses together with an older schist series (Oberc-Dziedzic *et al*., 2003*a*), and the Jegłowa Beds, corresponding to the Devonian quartzites of the Silesian domain (Oberc, 1966). All these rocks form the Strzelin Complex. In the Strzelin Massif, frag-

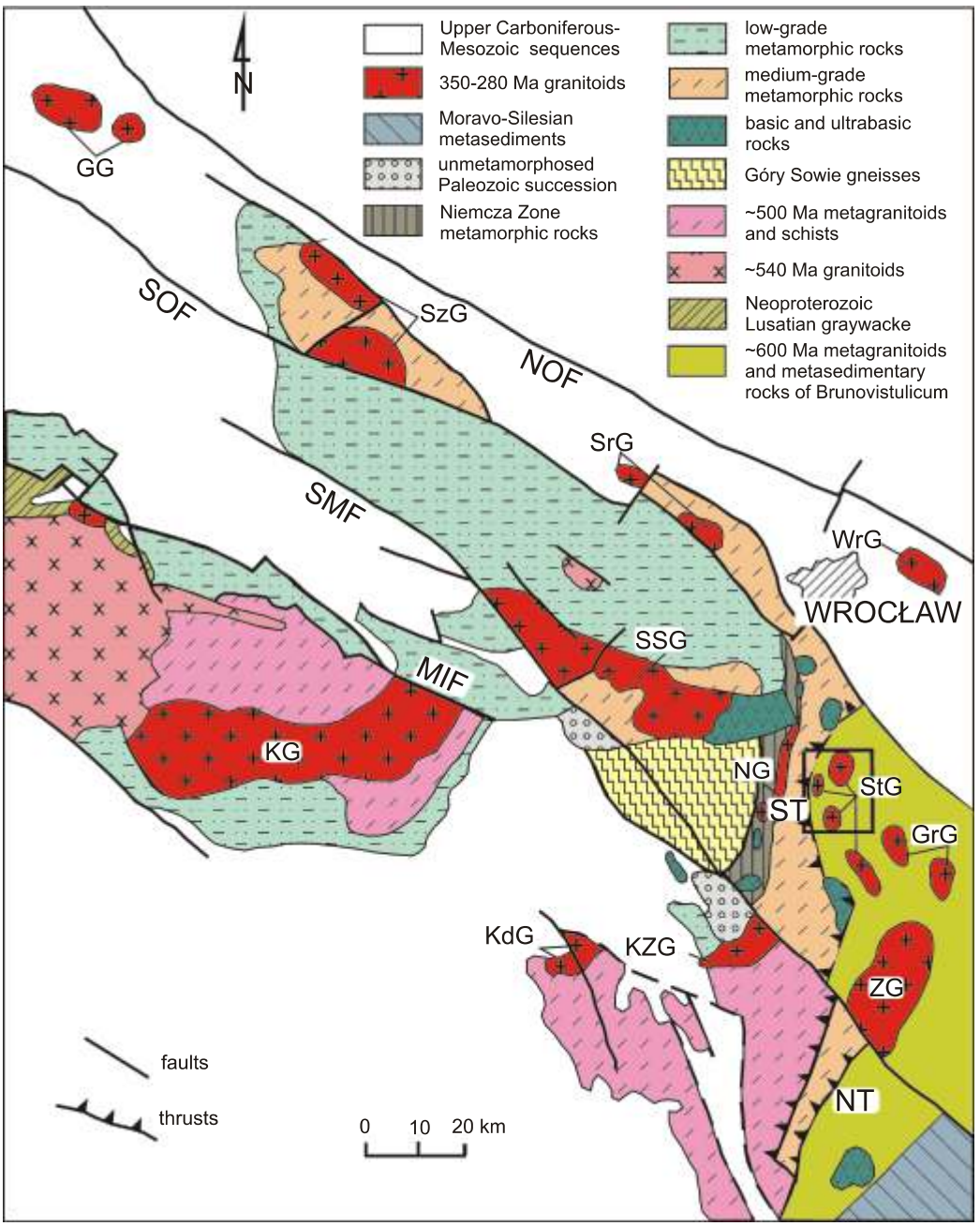

Fig. 1. Granitoids of the Sudetes, Fore-Sudetic Block and Odra Fault Zone

Variscan granitoids: Odra Fault Zone: GG – Gubin, SrG – Środa Śląska, SzG – Szprotawa, WrG – Wrocław; Fore-Sudetic Block: GrG – Grodków, NG – Niemcza, SSG – Strzegom–Sobótka, StG – Strzelin, ZG – Žulova; Sudetes: KdG – Kudowa, KG – Karkonosze, KZG – Kłodzko–Złoty Stok; faults: MIF – Main Intra-Sudetic Fault, SMF – Sudetic Marginal Fault, SOF – Southern Odra Fault, NOF – Northern Odra Fault; thrusts: NT – Nyznerov Thrust, ST – Strzelin Thrust; rectangle shows the position of the Strzelin Massif

ments of the Moldanubian Zone (Aleksandrowski and Mazur, 2002) also occur. They form small tectonic klippen separated from the rocks of Brunovistulicum by the Strzelin Thrust (Oberc-Dziedzic *et al*., 2005; Fig. 2). The klippen are composed of gneisses and schists of the Stachów Complex (Oberc-Dziedzic *et al*., 2005).

The collisional zones are often characterized by abundant granitic magmatism. In Brunovistulicum, Variscan granites are absent from its southern, Moravian part. In the NW part of the Silesian domain (Fig. 1), Variscan plutonic rocks form small bodies of pegmatitic muscovite granite, biotite granodiorite, pegmatite and hornblende-biotite-quartz monzodiorite (Cháb *et al*., 1994) and the relatively large Žulová Pluton composed of granite and tonalite (Cháb and Žaček, 1994). In the Strzelin Massif to the north, Variscan magmatism lasted about 30 m.y. and produced many small plutonic bodies, composed of

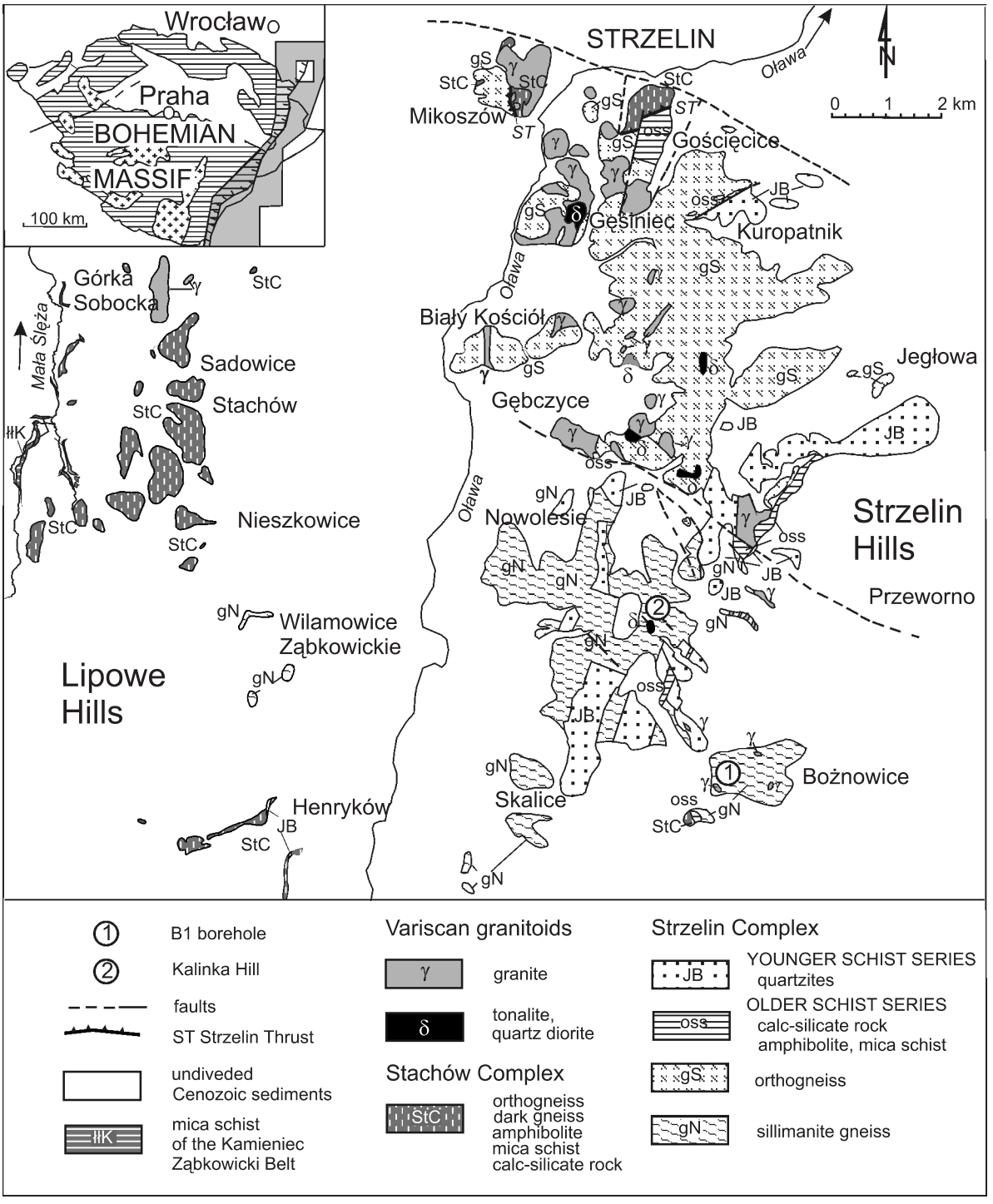

Fig. 2. Geological map of the Strzelin Massif (compiled by Oberc-Dziedzic and Madej, 2002, based on Oberc *et al.*, 1988; Wójcik, 1968; Wroński, 1973 and Badura, 1979)

The Strzelin Thrust plane separates the Stachów and Strzelin complexes. Inset map: Bohemian Massif and Moravo-Silesian Zone (grey-shaded); rectangle shows the position of the Strzelin Massif

dioritic-tonalitic and granitic rocks of various ages, structures and chemical features.

In this contribution, we present three stages of Variscan magmatism recognized in the Strzelin Massif, within the framework of its tectonothermal evolution.

GEOLOGICAL SETTING

The Strzelin Massif is situated in the eastern part of the Fore-Sudetic Block, 35 km south of Wrocław (Fig. 2). In the present paper, the name "Strzelin Massif" is used in a new, wider meaning: it comprises poorly exposed crystalline rocks

of the Lipowe Hills (western part of the massif, formerly the Lipowe Hills Massif) and crystalline rocks of the Strzelin Hills (eastern part of the massif, formerly the Strzelin Hills Massif) (Oberc-Dziedzic *et al*., 2005). The western and eastern parts of the Strzelin Massif are separated by a 6 km-wide belt of Cenozoic deposits. In the massif, two structural units, separated by the Strzelin Thrust (Oberc-Dziedzic and Madej, 2002; Oberc-Dziedzic *et al*., 2005), have been distinguished. The lower structural unit (the footwall of the thrust) belongs to Brunovistulicum, whereas the upper unit (the hanging wall) is considered as part of Moldanubicum (Oberc-Dziedzic and Madej, 2002; Oberc-Dziedzic *et al*., 2005). The rocks of the lower unit are more widespread in the eastern part of the Strzelin Massif, whereas those of the upper unit predominate in the western part of the massif.

The lower structural unit is composed of rocks of the Strzelin Complex, comprising gneisses, an older schist series, and a younger schist series (Fig. 2). The gneisses of the Strzelin Complex are represented by:

– the Strzelin orthogneiss – fine- to medium-grained, porphyritic biotite-muscovite gneiss, with conformable intercalations of amphibolites interpreted as former mafic dykes (Szczepański and Oberc-Dziedzic, 1998) and typical of the northern part of the Strzelin Massif; the Strzelin orthogneiss shows zircon ages of 600 ±7 and 568 ±7 Ma (Oberc-Dziedzic *et al*., 2003*a*);

– the Nowolesie gneiss – migmatic sillimanite gneiss, rich in pegmatites, but with no amphibolite intercalations, occurring in the southern part of the Strzelin and Lipowe hills, with late Neoproterozoic zircon ages (602 ±7 and 587 ±4 Ma, Klimas, 2008; 576 ±18 Ma, Mazur *et al*., 2010). Both the ages and geochemistry of the gneisses indicate their affinity to the Brunovistulian Terrane (e.g., Van Breemen *et al*., 1982; Kröner *et al*., 2000; Oberc-Dziedzic *et al*., 2003*a*; Mazur *et al*., 2010).

The older schist series (Oberc-Dziedzic and Madej, 2002; Oberc-Dziedzic *et al*., 2005) of unknown age is composed of amphibolites, mica schists, calc-silicate rocks and marbles. These rocks accompany the Strzelin orthogneiss and almost nowhere are in contact with the Nowolesie gneiss.

The younger schist series (the Jegłowa Beds; Oberc, 1966) consists of quartzites, quartz-sericite schists and metaconglomerates, the protoliths of which were interpreted to have been deposited in a back-arc basin during early- to mid-Devonian times (Szczepański, 2007). The Jegłowa Beds were correlated with the quartzite formation in the Jeseník Mountains of the East Sudetes (Bederke, 1931; Oberc, 1966), containing Early Devonian fossils (Chlupáč, 1975).

The upper structural unit (the hanging wall of the Strzelin Thrust) is a part of Moldanubicum (Aleksandrowski and Mazur, 2002) represented there by several tectonic klippen. It comprises the rocks of the Stachów Complex: dark, fine-grained paragneisses, as well as coarse-grained, porphyritic orthogneisses which have yielded late Cambrian/Ordovician (~500 ±5 Ma) zircon ages (Oliver *et al*., 1993; Kröner and Mazur, 2003; Oberc-Dziedzic *et al*., 2003*b*; Klimas, 2008; Mazur *et al*., 2010) typical of the Moldanubian Zone (e.g., Turniak *et al*., 2000) and Saxothuringian Zone (Oliver *et al*., 1993; Kröner *et al*., 2001; Oberc-Dziedzic *et al*., 2010). The intercalations of paragneisses, with mica schists and amphibolites, are interpreted as a Neoproterozoic or early Paleozoic metamorphic envelope of the granitoid protolith of the ~500 Ma orthogneisses (Oberc-Dziedzic and Madej, 2002).

The structure of the Strzelin Massif was formed during the Variscan orogeny in the course of two stages: the first, compressive stage that comprised D_1 and D_2 deformation events, and the second, extensional stage, comprising D_3 and D_4 events (Oberc-Dziedzic and Madej, 2002). The nape stacking, i.e. the formation of the Strzelin Thrust and thrust-bounded units of lower rank (Oberc, 1966; Cymerman, 1993; Oberc-Dziedzic, 1999), which took place during D_1, gave rise to crustal thickening and an increase in temperature. As a consequence, the gneisses of the southern part of the massif achieved anatectic conditions at T = 720°C and 6.5 ±1 kbar (Oberc-Dziedzic and Madej, 2002). The first stage of anatexis, after D_1 and during D_2, was followed by decompression related to the beginning of tectonic denudation. The decompression gave rise to the second stage of anatexis which produced pegmatites and leucocratic granites. The P-T conditions during the formation of the pegmatites were estimated as T = 600°C and P = 3 kbar based on a Grt + Bt + Sil + Ms assemblage (Oberc-Dziedzic and Madej, 2002). Subsequently, dome-like uplift of migmatized rocks took place (Oberc-Dziedzic and Szczepański, 1995; Szczepański and Mazur, 2004). The formation of the dome was accompanied by gravitational collapse (Szczepański, 2001).

The Strzelin and the Stachów complexes were intruded by four groups of Variscan granitoids (the numbers of the groups, 1 to 4, are referred to further in the text): (1) granodiorites, (2) tonalites and quartz diorites, (3) medium- and fine-grained biotite granites, and (4) two mica granites (Oberc-Dziedzic *et al*., 1996). The Strzelin Variscan granitoids are rather exceptional in the Sudetes area due to their petrographic variability and because they do not form a large single intrusion but many small isolated bodies, mostly stocks and flat veins, typically tens of metres thick (Oberc-Dziedzic, 1991). Their size and three-dimensional form were deduced from combining mapping data with structural observations, thermal aureoles and mutual relationships between granitoids and their metamorphic envelope in exposures and in a number of boreholes.

The granodiorites either form parts of granite and tonalite intrusions or separate bodies. In the former case, they are texturally similar to the granitoid dominating in the intrusion. In separate bodies, the granodiorites show a medium-grained texture, locally porphyritic, with parallel alignment of biotite, and some of them contain green hornblende. Field data show that the granodiorites (1) were emplaced in the Strzelin Massif at the begining of the Variscan igneous activity. The petrographic and geochemical features, as well as the ages of these rocks, are for the first time, presented in this paper.

The tonalites (2) are medium- or fine-grained rocks. They form small bodies which were emplaced in two magmatic events: first, at the begining of the Variscan plutonic activity, before the granodiorites (1), and second, at the end of that activity. The younger medium-grained tonalites exposed at Gęsiniec were examined in detail by Pietranik and Waight (2008); they were also dated at ~294 Ma using the Rb-Sr method (Pietranik and Waight, 2005) and 291 ±5.5 Ma by the Pb-evaporation zircon method (Turniak *et al*., 2006). The present paper provides new petrographic, geochemical and SIMS U/Pb zircon age data

for the oldest, medium-grained tonalites from Bożnowice, and for the younger fine-grained tonalites from Kalinka Hill in the southern part of the Strzelin Massif (Fig. 2).

The quartz diorites (of group 2) are dark, medium- and fine-grained rocks, often with black aggregates of hornblende and biotite. They form small bodies known mainly from boreholes. They have not been dated. The textures and mineral composition of the tonalites and quartz diorites change considerably within a magmatic body (Oberc-Dziedzic, 2007).

Group (3) of granitoids comprises medium-grained biotite granite and fine-grained biotite granite, together forming the largest intrusion in the Strzelin Massif (Oberc-Dziedzic, 2007). These rocks have been dated at 347 ±12 Ma (Rb-Sr whole rock method; Oberc-Dziedzic *et al*., 1996). A younger age of 301 ±7 Ma was obtained by Turniak *et al*. (2006) using the Pb-evaporation zircon method.

The pale, fine-grained biotite-muscovite granites (group 4) occur as dykes cross-cutting all types of granitoids or as separate intrusions. These rocks contain muscovite, andalusite and pinite pseudomorphs after cordierite (Bereś, 1969; Lorenc, 1987). The two mica granites were dated at 330 ±6 Ma (Rb-Sr whole rock method; Oberc-Dziedzic *et al*., 1996; Oberc-Dziedzic and Pin, 2000). However, bearing in mind that the two mica granites cut other granitoids in the massif, the Rb-Sr data should be rejected as too old in the light of the new ages reported for the biotite granites and tonalites.

The rocks studied here come from the southeastern part of the Strzelin Massif (Fig. 2). This part of the massif is composed of the Strzelin gneiss, with intercalations of amphibolite, mica schist and calc-silicate rock, which all were overthrust on the precursors of the Nowolesie gneiss during deformation D_1 (Oberc, 1966; Oberc-Dziedzic and Madej, 2002). The Variscan granitoids investigated comprise a granodiorite and medium-grained tonalite drilled in the B1 borehole near Bożnowice village, and a fine-grained tonalite exposed on Kalinka Hill in the southern part of the Strzelin Hills (Fig. 2). In the 240 m deep borehole B1, the granodiorite forms several bodies, 1–30 m thick, surrounded by gneiss and migmatite. The granodiorite contacts with the gneiss are sharp and both rocks often interfinger. The tonalite from the B1 borehole (the Bożnowice tonalite) forms two bodies, 0.5 and 1.5 m-thick in the borehole, surrounded by granodiorite (0.5 m-thick) and migmatized gneiss (1.5 m-thick). The contacts of the tonalite bodies with the granodiorite and gneiss are diffuse. In borehole B1, apart from the medium-grained tonalite, a fine-grained variety of tonalite occurs. It forms 2.5–11 m-thick bodies. The relationships between the two tonalite varieties are unclear. The fine-grained variety of tonalite and the fine-grained granite, cutting the gneiss and granodiorite, have not been examined in detail.

The Kalinka tonalite forms one of the largest tonalite bodies in the entire Strzelin Massif (Fig. 2). The body is a stock with a 60 m thick apophysis (Oberc-Dziedzic, 1991). The petrography of the Kalinka tonalite was described by Bereś (1969) and, more recently, by Białek (2006). Our studies of the Kalinka tonalite concentrated on the most widespread variety dated here by the SHRIMP method.

ANALYTICAL METHODS

The samples of granitoids and country rocks for petrographic and geochronological studies were taken from borehole B1 situated north of Bożnowice village in the southeastern part of the Strzelin Massif, and from a small exposure on Kalinka Hill in the central part of the massif (Fig. 2).

The petrographic observations are based on 36 thin sections examined under the polarizing microscope. The chemical composition of rock-forming minerals was analysed at the Inter-Institute Analytical Complex for Minerals and Synthetic Substances, Electron Microprobe Laboratory, Faculty of Geology, the University of Warsaw. Analyses on 5 specimens were carried out with the *CAMECA SX 100* instrument, at the acceleration voltage 15 kV, the electron beam current 10 nA for analyses of plagioclase and mica, and 20 nA for other minerals, and at counting time 20 s. The standards included both the minerals and synthetic substances. The raw data were processed with the *PAP* software supplied by *CAMECA*.

Six rock samples (Table 1) were analysed for major, trace and rare earth elements, using combined ICP-OES and ICP-MS techniques (Actlabs, Canada, code "4Lithores").

One sample of granodiorite and 2 samples of tonalite have been analysed by C. Pin (University Blaise Pascal, Clermont-Ferrand) for Sm-Nd isotopes, following procedures described by Pin and Santos Zalduegui (1997). The analytical data are listed in Table 2 (data from Oberc-Dziedzic *et al*., 2009*b*). The initial $^{143}Nd/^{144}Nd$ ratios are expressed as εNd_i values, corrected for *in situ* decay of ^{147}Sm, assuming an age of 305 Ma for the granodiorite, 325 Ma for the Bożnowice tonalite, 295 Ma for the Kalinka tonalite, and with model ages relative to the depleted mantle model of De Paolo (1981*a*, *b*).

Three samples have been selected for SHRIMP zircon dating: B1 188.2 – medium-grained tonalite, Bożnowice, borehole B1; B1 117.5 – medium-grained granodiorite, Bożnowice, borehole B1; and KAL – fine-grained tonalite from Kalinka Hill (Fig. 2). These samples, each *ca*. 5 kg in weight, were crushed and the heavy mineral fraction (0.06–0.25 mm) separated using a standard procedure with heavy liquid and magnetic separation. Zircons were handpicked under a microscope, mounted in epoxy resin and polished. Transmitted and reflected light photomicrographs were made along with CL and BSE images in order to select grains and choose sites for analysis. The Sensitive High Resolution Ion Microprobe (SHRIMP II) at the All-Russian Geological Research Institute (VSEGEI) in St. Petersburg was used to determine zircon ages in the samples selected. Overall, 22 analyses in each of the three samples were performed.

SHRIMP analytical details are given in the Appendix. Uncertainties for individual analyses (ratios and ages) are at the one σ level; however, the uncertainties in calculated Concordia ages are reported at the 2 σ level. The results of the zircon analyses are shown in Tables 3–5, and in Figures 8–13.

Documentation of the research (samples, thin sections, results of whole-rock, EMP and other analyses, and the photo documentation) are in the possession of the authors.

Table 1

Chemical analyses of granodiorite and tonalite from borehole B1 and of the Kalinka tonalite

[%]	Granodiorite		Tonalite			
	B1 92	B1 92J	B1 188J	B1 188.2	K2c	KAL
SiO_2	69.59	68.97	62.57	61.36	58.25	59.16
TiO_2	0.37	0.38	0.764	0.9	1.16	1.15
Al_2O_3	15.87	16.3	13.79	15.7	17.04	16.54
Fe_2O_3	2.53	2.23	5.96	6.45	7.23	6.98
Cr_2O_3	<0.002	0.001		0.018	0.008	0.009
MnO	0.04	0.03	0.117	0.1	0.11	0.11
MgO	0.88	0.82	4.11	3.91	3.32	3.28
CaO	2.48	2.45	7.25	4.64	5.61	5.47
Na_2O	4.01	3.99	1.74	2.32	3.35	3.29
K_2O	3.15	3.46	1.99	2.49	2.44	2.38
P_2O_5	0.01	0.02	0.42	0.32	0.42	0.41
LOI	0.7			1.5	1	0.9
Total	**99.64**	**98.65**	**98.71**	**99.68**	**99.94**	**99.71**
A/CNK	1.1	1.1	0.8	1	0.9	0.9
A/NK	1.6	1.6	2.7	2.4	2.1	2.1
ppm						
Cu			170.5	65.5	28.9	22.5
Pb	4	5		2.4	2.7	1.6
Zn	38	36	46	53	75	63
Ni			45	31.6	18.5	17.7
Au				<0.5	10.9	0.5
Tl	0.4	0.3	0.3	0.4	0.4	0.4
Ba	1502	1627	461	651	513.1	551
Co	74	97	26	65.5	82.5	52.2
Cs	3.8	3.9	2.0	2.7	1.6	1.6
Ga	17.3	17.4	20	20.8	21.1	21.6
Hf	4.6	4.1	7.4	8.6	7.8	8
Nb	8.4	7.8	18.1	22.7	25.1	28
Rb	101	99	83	101.7	82.7	91.8
Sn	2	2	2	3	3	3
Sr	599	594	292	292.6	317.5	333.5
Ta	0.6	0.5	2.7	1.4	1.8	1.6
Th	2.1	2.7	14.5	11.3	10.5	7.9
U	1.8	1.7	5.32	6.1	1.6	1.9
V	32	30	87	98	116	128
Zr	148	130	312	335.6	316.6	346.6
Y	3.9	3.3	33.0	29.9	35.9	34.4
La	5.9	7	71.0	43.7	55.1	42.6
Ce	9.4	11	132	90.9	114.8	87.5
Pr	0.97	0.95	15.0	11.4	12.48	11.61
Nd	2.7	3.6	55.3	40.3	46.3	41.7
Sm	0.34	0.6	10.2	7.45	9.3	8.19
Eu	0.92	1.31	1.86	1.45	2.01	1.97
Gd	0.41	0.33	8.36	5.83	7.67	7.03
Tb	0.07	0.07	1.26	0.95	1.25	1.1
Dy	0.14	0.56	6.5	5.28	6.27	6.24
Ho	0.12	0.1	1.27	0.99	1.25	1.18
Er	0.43	0.38	3.33	2.87	3.37	3.32
Tm	0.08	0.08	0.51	0.43	0.51	0.48
Yb	0.48	0.53	3.03	2.6	2.72	2.94
Lu	0.1	0.09	0.44	0.42	0.44	0.45
Σ REE	22.06	18	310.06	214.57	263.47	216.31
La_N/Yb_N	8.22	8.83	15.69	11.2	13.55	9.7
Eu/Eu*	7.57	9.05	0.62	0.68	0.73	0.8

A/CNK A = mol Al_2O_3, C = mol CaO, N = mol Na_2O, K = mol K_2O, CNK = C + N + K, NK = N + K

PETROGRAPHY

COUNTRY ROCKS

Orthogneiss from the Bożnowice region, being the country rock for the Variscan granitoids, is known from several exposures and from two boreholes (B1 and B2). It is a pale grey, fine-grained rock, with microcline porphyroblasts in places, showing a clearly visible foliation defined by layers of quartz and plagioclase-microcline and biotite streaks. The polygonal shapes of quartz and feldspar grains, abundance of sillimanite, presence of intergranular film of albite and myrmekite, together with rare leucosome and more often with biotite-rich selvages of melanosome (up to 20 mm-thick), parallel foliation, all are suggestive of high temperature metamorphic conditions and an incipient stage of migmatization. At the contact with granodiorite and migmatite, the gneisses lose their foliation and become very fine-grained, nearly aphanitic.

Migmatites (sample B1 89.5) form rare intercalations within the gneiss. At the contacts with the granodiorite, the migmatites are enriched in plagioclase and quartz-feldspar veins, whereas the granodiorite often contains scraps of migmatite. The migmatites are composed of 1.0–1.5 cm lenticular domains of quartz and similar-sized very fine-grained domains of quartz-plagioclase, with minor biotite. Locally, the plagioclase of such domains forms larger grains hosting chaotically arranged bunches of sillimanite. Biotite accompanied by such plagioclase does not show any signs of transformation. Both types of domain are surrounded by packets of coarse-grained biotite. Locally, the migmatites grade into biotite schists (sample B1 89.7) with clearly visible foliation defined by biotite and bunches of sillimanite. Small plagioclase and rare microcline grains occur among the quartz grains. The mica schists contain also prismatic sillimanite and late muscovite, the latter being a product of plagioclase and sillimanite alteration.

In the migmatites, larger, rounded plagioclase grains, 1–3 mm in diameter, form clusters or single crystals surrounded by biotite. They contain 38–46% An in the core and 22–26% An in the rim. The cores are irregular and embayed. The large plagioclase grains contain inclusions of small rounded flakes of biotite. The composition of small rounded plagioclases from very fine-grained domains, and of larger anhedral grains associated with sillimanite, is the same as that of the rims of the large plagioclase grains, i.e. 23–27% An.

Table 2

Sm-Nd isotope data for granodiorite and tonalie from borehole B1 and for the Kalinka tonalite (data from Oberc-Dziedzic *et al.*, 2009*b*)

	Sample	Type	Sm	Nd	Sm/Nd	$^{147}Sm/^{144}Nd$	$^{143}Nd/^{144}Nd$	εNd_0	$\varepsilon Nd_{(t)}$	Age (t) [Ma]	T_{CHUR}	T_{DM} [Ga]
1	B1 92.3	granodiorite Bożnowice	0.527	3.87	0.14	0.0823	0.512015 (2)	–12.2	–7.7	305	1.20	1.20
2	B1 188.2	tonalite Bożnowice	7.65	41.6	0.18	0.1111	0.512236 (2)	–7.9	–4.3	325	0.72	1.20
3	KAL	tonalite Kalinka	7.96	42.3	0.19	0.1136	0.512275 (2)	–7.1	–4.0	295	0.67	1.17

T_{CHUR} – T-Chondritic Uniform Reservoir model ages; T_{DM} – T-Depleted Mantle model ages

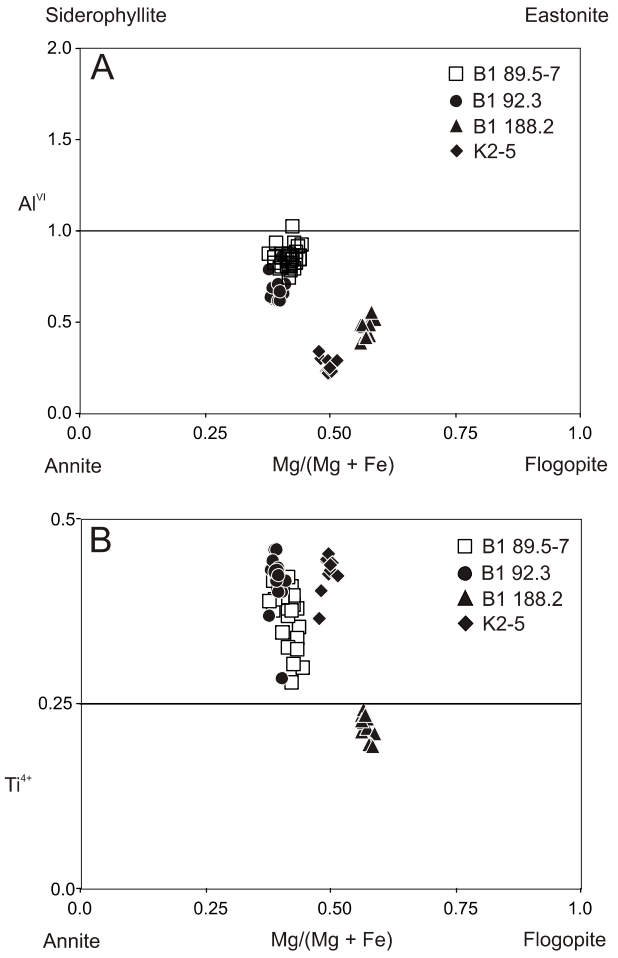

Fig. 3. Composition of biotite from the Bożnowice migmatite, granodiorite and tonalite and from the Kalinka tonalite

A – Mg/(Mg+Fe) vs. Al^{VI}diagram; **B** – Mg/(Mg+Fe) vs. Ti^{4+}diagram

K-feldspar was detected using EPMA as very rare small grains hidden among plagioclases in the matrix. It contains up to 10.6% of Ab and 2.3% Cs components but practically no An.

Coarse-grained biotite is characterized by constant Mg/(Mg + Fe) ratios of ~0.43 (Fig. 3). The Ti^{4+}content in this kind of biotite is distinctly higher and Al^{VI} is lower than in biotites enclosed in larger plagioclases from the very fine-grained domains (respectively: Ti^{4+}: 0.32 to 0.42 apfu vs. 0.29; Al^{VI}: ~0.85 apfu vs. ~1.0 apfu). The very fine-grained domains probably formed during incipient melting.

GRANODIORITE

Sample B1 92.3 is a medium-grained granodiorite composed of quartz, plagioclase, K-feldspar and biotite. Pale grey-bluish K-feldspar phenocrysts, up to 1 cm across, are rare.

The K-feldspar grains consist of the core, rich in Ab (up to 15%) and Cs (up to 3.6%) components (Fig. 4A), and the zoned rim, reflecting variable Ba contents (Fig. 4A). In places, a thin zone of tiny inclusions of feldspar of $Or_{56.7}$-$Ab_{31.6}$-$An_{10.7}$-$Cs_{1.0}$ is visible between the core and rim. K-feldspar grains contain inclusions of plagioclase, biotite, ilmenite and quartz in their inner parts (Fig. 4A), but rims are free of inclusions, except the borders, that contain inclusions of plagioclases of ~27% An formed by the corrosion of plagioclase by K-feldspar (Fig. 4B). In the matrix, K-feldspar forms small anhedral grains among rounded plagioclase (Fig. 4C).

Plagioclase forms two types of grain: larger, tabular crystals, several mm long, locally deformed (Fig. 4D), and smaller rounded grains (Fig. 4E), enveloped by biotite. Both types have corroded cores containing 40–51% An (46% in rounded grains) and rims, in which An content decreases from 35% An in the inner part to 26% at the margin. Between the cores and rims, there is a zone containing 26–30% An (Fig. 4D, E). Plagioclase forms also inclusions in K-feldspar. In such inclusions, the inner parts, containing 22–25% An, are surrounded by rims of pure albite. A similar composition is observed in perthitic intergrowths in K-feldspar phenocrysts. Small grains in the matrix contain about 28% of An (Fig. 4C), similarly as rims of larger grains.

Biotite in the granodiorite has a very constant composition. The Ti^{4+} content is usually within the range of 0.40–0.46 apfu, Al^{VI} is 0.60–0.70 apfu, exceptionally higher (Fig. 3). The composition field of the biotite from the granodiorite partly overlaps those from migmatites and mica schists (Fig. 3).

TONALITES

The Bożnowice tonalite is a dark grey, medium-grained rock, homogenous in the inner part of the intrusion, and showing schlieren structure towards the contact with the country rocks. The matrix displays a hipidiomorphic texture, defined by plagioclase laths. Apart from the small plagioclases, larger grains of that mineral, with older cores, are spotted. In places, they form clusters surrounded by a common rim. Dark minerals, biotite and amphibole, form separate monomineral clusters. Commonly, the amphibole clusters are overgrown by biotite.

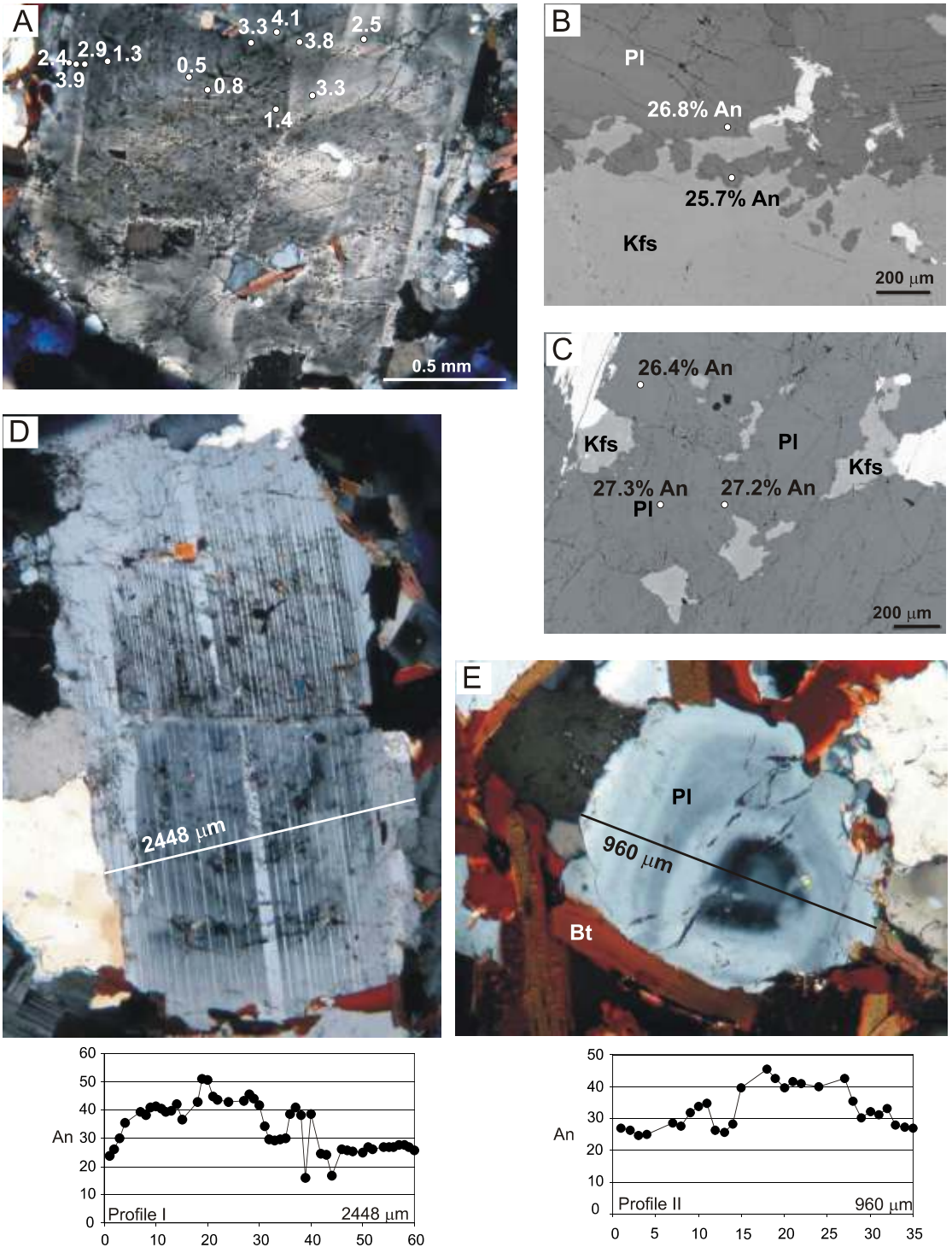

Fig. 4. Minerals of granodiorite B1 92.3

A – zoned K-feldspar phenocryst, numbers show celsian content, crossed polars; **B** – corrosion of plagioclase (Pl) by K-feldspar (Kfs), BSE image; **C** – anhedral grains of Kfs among rounded plagioclase grains (Pl) of the matrix, BSE image; **D** – cracked grain of plagioclase (Pl), crossed polars, below: profile showing An content; **E** – rounded plagioclase grain surrounded by biotite (Bt), crossed polars, below: profile showing An content

The Kalinka tonalite is a fine-grained rock composed of euhedral laths of plagioclase, 0.5–1 mm in size, defining a hipidiomorphic texture, and of quartz, amphibole, biotite and apatite. K-feldspar forms rare minute grains.

A common feature of the plagioclase of the Bożnowice and Kalinka tonalites is the presence of a cleft at the border between the inner and outer parts of a grain (Fig. 5A–D, F). This cleft is usually empty, but can be filled with pyrite (Fig. 5F). Larger (up to 2 mm) grains of plagioclase in the Bożnowice tonalite display euhedral inner parts and irregular, zoned rims (Fig. 5A, B). The inner parts contain a dismembered and embayed core, with up to 76% An, rimmed by 38–42% An plagioclase (Fig. 5B, profile

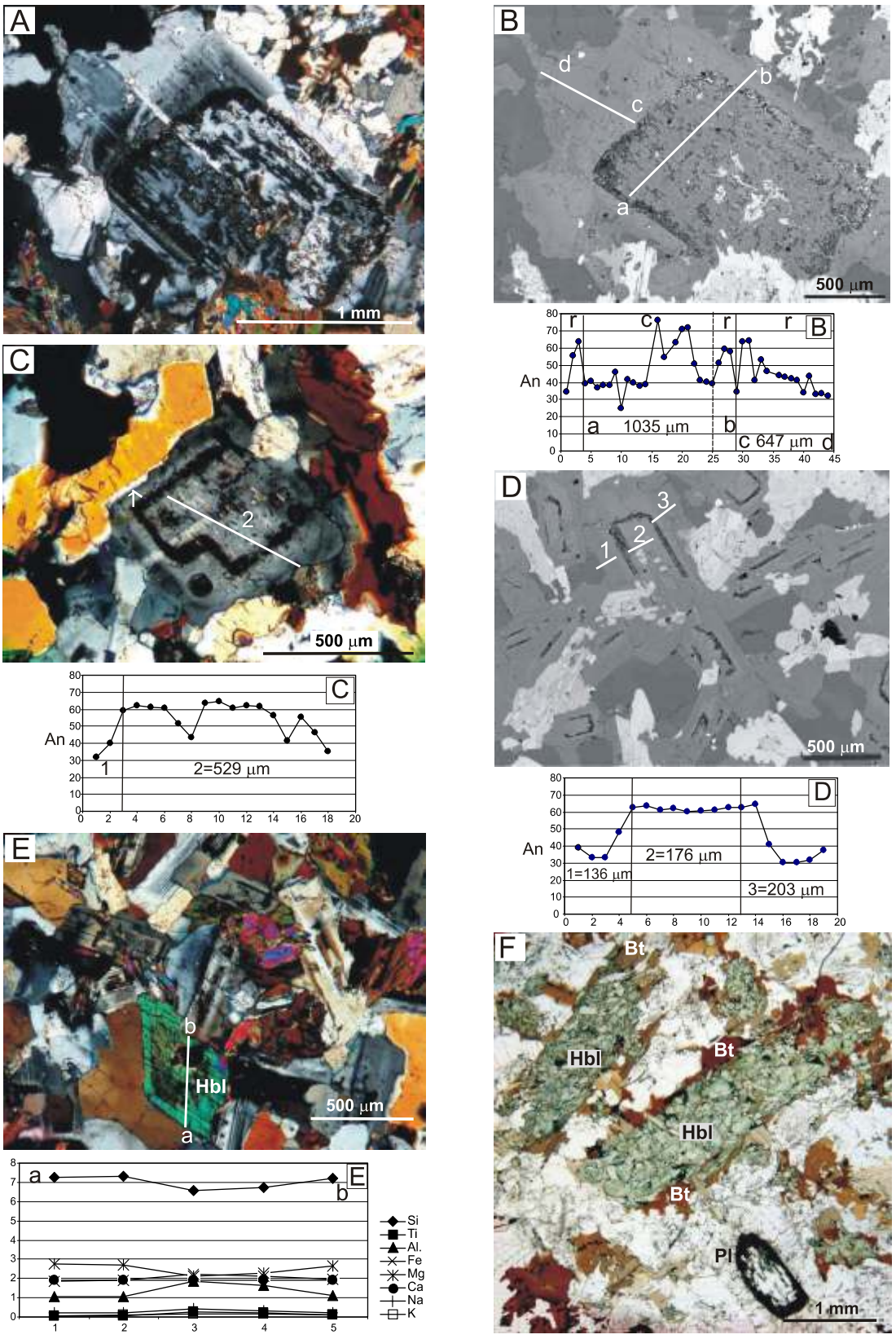

Fig. 5. Minerals of tonalites

A – plagioclase from B1 188.2 tonalite, crossed polars; **B** – the same grain as (A) in BSE image; below: profiles a–b and c–d showing An content in plagioclase, r – rim, c – core; **C** – plagioclase twins in Kalinka tonalite K2-5, crossed polars; below: profiles 1 and 2 showing An content in plagioclase; **D** – BSE image of plagioclases in Kalinka tonalite with hipidiomorphic texture; below: profile 1, 2, 3 showing An content in one of grains; **E** – euhedral grain of hornblende (Hbl) in Kalinka tonalite; below: compositional profile (a–b) of hornblende; **F** – B1 188.2 tonalite: two pseudomorphs after amphibole composed of small grains of magnesiohornblende (Hbl), surrounded by biotite (Bt); at the bottom, plagioclase grain (Pl) with the core surrounded by a cleft filled with pyrite; similar clefts but not filled, are visible also on A–D, one polar

a–b, c part on the graph). The An content occasionally decreases to ~25% An (Fig. 5B – graph). In the outer part, the An content near the cleft increases up to 64% and sharply (left side of graph Fig. 5B) or gradually decreases to 32% (c–d profile, right side of graph, Fig. 5B). Small anhedral laths of plagioclase from the matrix of the Bożnowice tonalite have the same content of An as the outer parts of larger grains, i.e. up to 64% An in the cores, and 26–35% An in the rims.

In the Kalinka tonalite, the An content in the inner parts of plagioclases is only slightly variable, between 64% An and 61% An (Fig. 5C, D). In the outer parts, outside the clefts, the An content decreases from 62 to about 30% and then increases to 37% (Fig. 5D graph).

The large plagioclase grains in the Kalinka tonalite show simple zonation patterns, compared with the complex ones in the Bożnowice tonalite. The composition of the Kalinka plagioclases and the rims of the larger plagioclase grains and small matrix grains in the Bożnowice tonalite are similar.

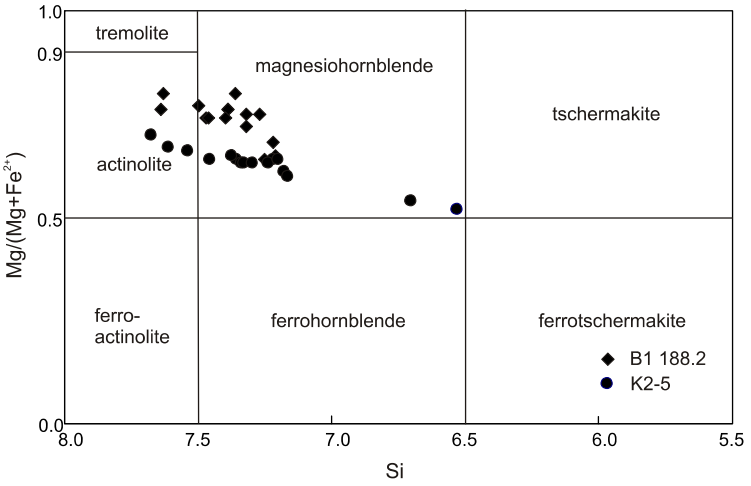

Fig. 6. Compositional variation of amphiboles from Bożnowice and Kalinka tonalites shown on the Leake *et al*. (1997) classification diagram; 31 analyses

In both types of tonalite, biotite forms clusters and single plates, or overgrowths on amphibole clusters. The chemical composition of the biotite does not depend on its position in the rock. The Mg/(Mg + Fe) ratios of biotites in the Bożnowice tonalite are higher compared with those in the Kalinka tonalite. Both tonalites have these ratios higher than the granodiorite and migmatite. The biotites in the Kalinka tonalite are richer in Ti (0.36–0.45 apfu) compared with the Bożnowice tonalite (0.19–0.24 apfu). In contrast, the Al^{VI}content is higher in the biotite from the Bożnowice tonalite (0.38–0.51 apfu) than that from the Kalinka tonalite (0.22–0.34 apfu) (Fig. 3).

In both types of tonalite, amphiboles usually form clusters of small, pale green grains (Fig. 5F). The euhedral grains are only occasionally found in the Kalinka tonalite (Fig. 5E). Following the procedure of Leake *et al*. (1997), the amphiboles in the Bożnowice and Kalinka tonalites belong to the calcic group, with Ca_B >1.5, $(Na + K)_A$ <0.50 and Ca_A <0.50. In both tonalites, the amphiboles are actinolite and magnesiohornblende, with Mg/(Mg + Fe) ratios 0.64–0.80 in the Bożnowice tonalite, and 0.57–0.70 in the Kalinka tonalite (Fig. 6). The cores of the larger, euhedral amphibole grains from the Kalinka tonalite show much higher contents of Al, Na, K, Ca and Ti, and lower contents of Si than the small anhedral amphibole grains. Their composition is close to tschermakite (Fig. 5E, graph; Fig. 6).

BULK-ROCK CHEMISTRY

MAJOR ELEMENTS IN GRANODIORITE AND TONALITES

The Bożnowice granodiorite (B1 92) is a silica-rich (69% SiO_2) and potassium-rich (3.15–3.46% K_2O), peraluminous rock, with A/CNK of 1.1 (Table 1), and relatively high, up to 1.4%, contents of normative corundum. The proportion of normative orthoclase (28%) and normative plagioclase (Ab + An ~ 46%) is typical of granodiorite. The Bożnowice (B1 188) and the Kalinka (K2c, KAL) tonalites show small but distinct differences in the major element contents. The Bożnowice tonalite is richer in SiO_2 and MgO but poorer in TiO_2, Al_2O_3, Fe_2O_3, K_2O and Na_2O than the Kalinka tonalite. Both tonalites are high potassic, metaluminous rocks with A/CNK 0.8–1.0 (Table 1).

TRACE AND RARE EARTH ELEMENTS IN GRANODIORITE

The Bożnowice granodiorite is very rich in Ba (1500–1627 ppm) and Sr (~600 ppm). Ba contents are 200–600 ppm higher and Sr about 200 ppm higher than in other granodiorites in the Central and East Sudetes (Oberc-Dziedzic *et al*., 2009*b*). The Zr/Nb (16.66–17.62), Nb/Th (2.88–4.0) and Ce/Pb (2.2–2.35) ratios are comparable with those of the continental crust (Hofmann, 1988; Wedepohl *et al*., 1991; Nutman *et al*., 1999; Oberc-Dziedzic *et al*., 2009*a*).

The multi-element diagram of trace element concentrations normalized to chondrite (Fig. 7A) is characterized by strong Th and P negative anomalies and strong positive anomalies of Sr, Zr and Hf; however, there are no negative anomalies of Nb and Ta, usually considered as typical of continental crust material (Taylor and McLennan, 1985). The negative phosphorus anomaly reflects probably apatite fractionation and removal or scarcity of this component in the source materials.

In the Bożnowice granodiorite, the total REE content is very low, 18–22 ppm (Table 1). The chondrite-normalized REE patterns (Fig. 7B) display distinct, steep decreasing LREE and slightly increasing HREE branches, apparently indicating specific chemical characteristics of the magma source. The $(La/Yb)_N$ ratios are 8.22–8.83. The most characteristic feature of the granodiorite REE patterns is a pronounced positive anomaly of Eu/Eu*, between 7.57–9.05, indicating that this rock contains substantial amounts of cumulus plagioclase, also clearly seen in the high Sr contents.

The enrichment of the granodiorite in Ba, Sr and Eu (in proportion to La and Y), all suggest feldspar fractionation processes.

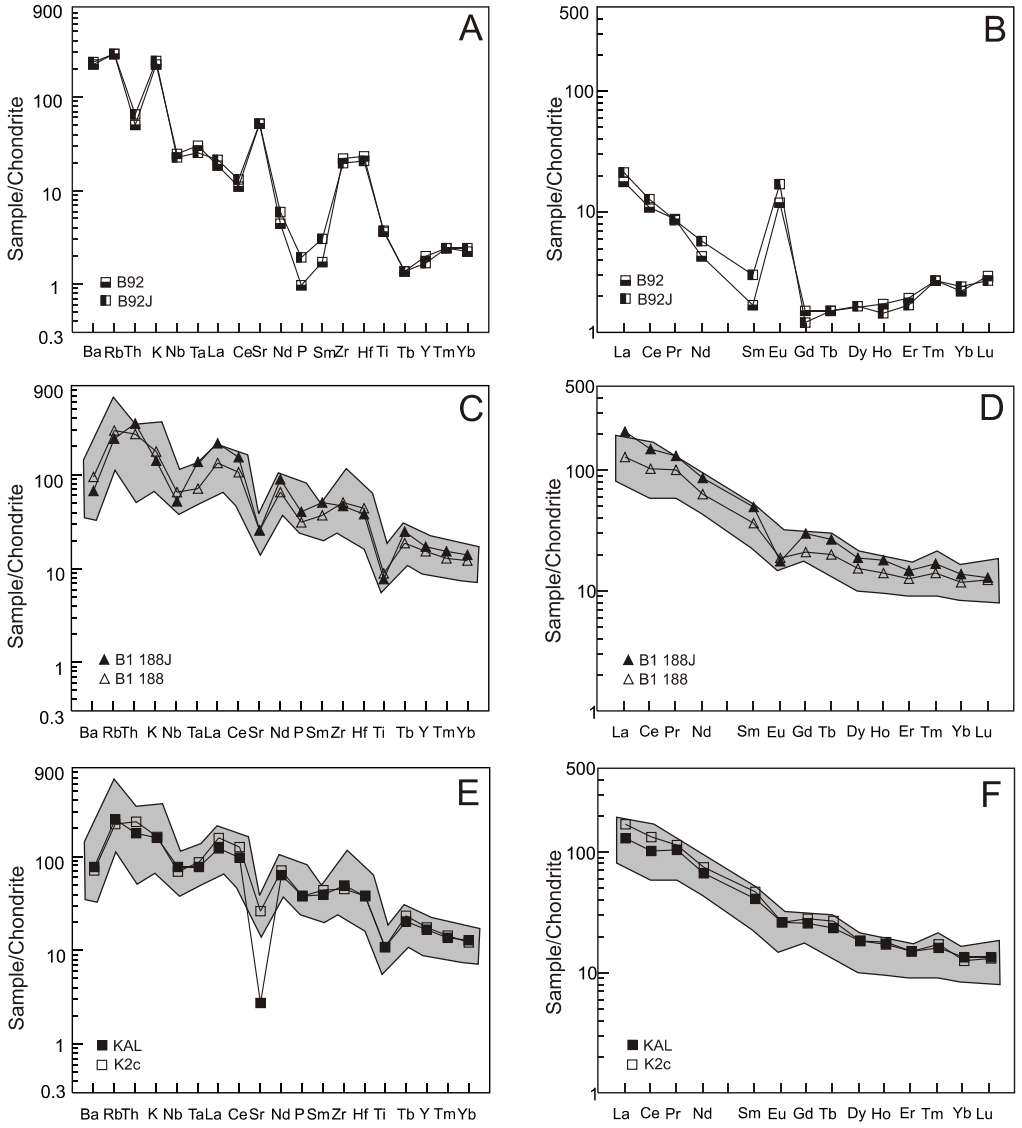

Fig. 7. Bożnowice granodiorite (A, B), Bożnowice tonalite (C, D) and Kalinka tonalite (E, F) compared with 7 samples of the tonalites ~295 Ma (shaded) from the Strzelin Massif on the chondrite-normalized multi-element diagrams – A, C, E (normalization values of Thompson, 1982) and chondrite-normalized REE plots – B, D and F (normalization values of Nakamura (1974) with additions from Haskin *et al.*, 1968)

TRACE AND RARE EARTH ELEMENTS IN TONALITES

The Bożnowice tonalite and the Kalinka tonalite display similar concentrations of trace elements, except Ni, U and Cu, which are much higher in the Bożnowice tonalite than in the Kalinka tonalite (respectively, Ni: 31.6–45 and 17.7–18.5; U: 5.32–6.1 and 1.6–1.9, Cu: 65.5–170.5 and 22.5–28.9 ppm; Table 1). On the diagrams of trace element concentrations normalized to chondrite (Fig. 7C, E), all tonalite samples show negative Nb, Sr and Ti anomalies. The Nb anomaly is considered as typical of continental crust (Taylor and McLennan, 1985). The distinct negative Sr anomaly (Fig. 7C, E) reflects the low concentration of this element in the tonalites (292–333 ppm) compared with that in chondrite (11 800 ppm; Thompson, 1982), but similar to that in upper crust (350 ppm; McLennan *et al.*, 2006). The Sr, P and Ti negative anomalies point, respectively, to plagioclase, apatite, and ilmenite fractionation and removal. The combined negative Eu- and Sr anomalies suggest that plagioclase was either an important residual mineral in the source or was (partly?) removed during fractional crystallization (Green, 1980).

The absolute abundances of total REE in the Bożnowice and Kalinka tonalites are much higher (214–310 ppm) than in the granodiorite. The patterns on the plot of REE normalized to chondrite (Fig. 7D, F) are characterized by an enrichment of light REE and a flat, nearly horizontal HREE section. The enriched LREE section indicates moderate fractionation of the lightest REE (up to ~200 times chondrite values for La). The $(La/Yb)_N$ ratios are 9.7–15.69. The fairly flat HREE sector may indicate the presence of pyroxene and/or hornblende in the source (Hanson, 1978). The tonalites have a small negative Eu anomaly (Eu/Eu* = 0.62–0.8).

The patterns of chondrite-normalized trace and REE diagrams of the Bożnowice and Kalinka tonalites are similar to the patterns of other tonalites from the Strzelin Massif (Fig. 7C–F).

Sm-Nd SYSTEMATICS

The Sm-Nd isotope ratios in the Bożnowice granodiorite and the Bożnowice and Kalinka tonalites are given in Table 2 (data from Oberc-Dziedzic *et al*., 2009*b*). The Bożnowice granodiorite displays the lowest values of all ratios: Sm/Nd (0.14), $^{147}Sm/^{144}Nd$ (0.0823), $^{147}Nd/^{144}Nd$ (0.512015), and εNd_{305}(–7.7). The model age calculated using the De Paolo (1981*a*, *b*) depleted mantle model (T_{DM}) is 1.2. In both types of tonalites, all these ratios (except the T_{DM} values) are higher than in the granodiorite (Table 2) and similar to each other. The negative εNd value indicates a likely crustal source of magma. The higher values of εNd_{325}= –4.3 in the Bożnowice tonalite and of εNd_{295}= –4.0 in the Kalinka tonalite might reflect igneous mixing, in adequate proportions, of typical continental material with negative εNd values, and mafic magma with positive εNd.

SHRIMP ZIRCON STUDY

BOŻNOWICE TONALITE, SAMPLE B188.2

All the zircons in this sample are alike: subhedral to anhedral, with a specific, "corroded" appearance. In reflected light, in many crystals, numerous "cavities" are visible. In cathodoluminescence (CL) images (Fig. 8), all the grains show very characteristic internal structures: radial or fan-like patterns of alternating CL-darker and brighter, often diffused stripes. Such structures could result from metamictization. An important role of metamictization processes in these zircons is in line with the observed high U (882–5807 ppm) and, often, Th (50–5192 ppm) contents (Table 3). The Th/U ratio varies between 0.02 and 2.09, and the $^{206}Pb_c$ is usually low, 0.0–1.14%.

Six points analysed have significant discordance D, between +10 and +68%, suggesting that the $^{207}Pb/^{206}Pb$ ages, scattered from 340 to 480 Ma, represent minimum ages (Table 3). The remaining 16 points are broadly concordant and their mean Concordia age is 324 ±4 Ma (Fig. 9). Four points (9.1, 4.1, 19.1 and 19.2) intercept at 0 and 331 ±12 Ma.

Summing up, the main zircon population of 324 ±4 Ma mean Concordia age could be interpreted as representing the main magmatic event. However, the positively discordant points may indicate Pb-loss (and lowering the Th/U ratios), thus possibly implicating that the true magmatic age may be older, e.g. corresponding to the oldest points of the main population, around 330 Ma.

BOŻNOWICE GRANODIORITE, SAMPLE B1 117.5

The zircon population in this sample is homogeneous and represented by euhedral, long- to normal-prismatic, clear and transparent crystals. A few grains are broken. Most of the crystals in CL images display strong oscillatory, magmatic zonation. In a few grains, CL-bright or cloudy cores are visible (Fig. 10).

The U and Th concentrations vary from low (U 72 ppm, Th 24 ppm), to rather high (e.g., U 1703 ppm, Th 812 ppm). The Th/U ratio varies slightly, between 0.22 and 1.14, whereas $^{206}Pb_c$ is low, 0.02–1.13% (Table 4).

Two analytical points show relatively high negative discordance (point 10.1 –57; point 1.1 –22), and they should be interpreted with caution. Three other points clearly indicate the

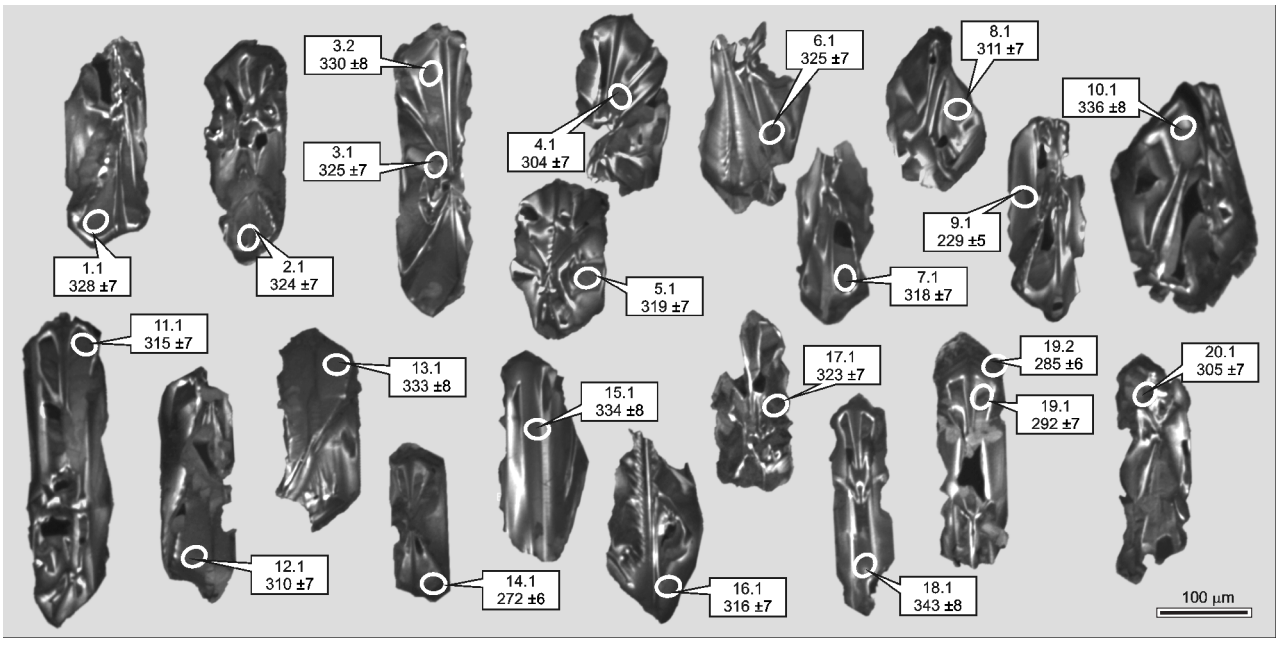

Fig. 8. Cathodoluminescence images of zircons analysed from Bożnowice tonalite B1 188.2

Various morphological types and various internal structures are represented (see text for further explanation). Symbols of analytical points correspond to those in Table 3; analytical points indicated by elipses, with longer axis *ca.* 30 µm; $^{206}Pb/^{238}U$ ages and one errors are given

Table 3

SHRIMP data for zircons from the Bożnowice tonalite, sample B1 188.2

Spot	$^{206}Pb_c$ [%]	U [ppm]	Th [ppm]	$^{232}Th/^{238}U$	$^{206}Pb^*$ [ppm]	(1) $^{206}Pb/^{238}U$ Age		(1) $^{207}Pb/^{206}Pb$ Age		(1) $^{208}Pb/^{232}Th$ Age		Discordant [%]	Total $^{238}U/^{206}Pb$	±%	Total $^{207}Pb/^{206}Pb$	±%	(1) $^{238}U/^{206}Pb^*$	±%	(1) $^{207}Pb^*/^{206}Pb^*$	±%	(1) $^{207}Pb^*/^{235}U$	±%	err corr
B1 188.2 1.1	–	1667	32	0.02	74.8	328.2	±7.9	322	±19	346	±26	–2	19.15	2.5	0.05282	0.83	19.15	2.5	0.05283	0.83	0.3805	2.6	0.949
B1 188.2 2.1	0.23	1954	823	0.44	87	324.9	±7.8	337	±33	331.5	±9.5	4	19.3	2.5	0.05508	0.91	19.35	2.5	0.05319	1.5	0.379	2.9	0.86
B1 188.2 3.1	–	1620	671	0.43	72	325.2	±7.9	340	±23	350	±11	4	19.33	2.5	0.05321	1	19.32	2.5	0.05325	1	0.38	2.7	0.926
B1 188.2 3.2	0.00	1584	181	0.12	71.6	330.7	±8	324	±23	342	±11	–2	19	2.5	0.05289	1	19	2.5	0.05289	1	0.384	2.7	0.924
B1 188.2 4.1	0.22	1356	64	0.05	56.5	304.4	±7.4	378	±47	333	±51	24	20.64	2.5	0.05597	1.1	20.68	2.5	0.0542	2.1	0.361	3.3	0.763
B1 188.2 5.1	0.03	1258	72	0.06	55	319.8	±7.7	336	±27	352	±16	5	19.66	2.5	0.05343	1.2	19.66	2.5	0.05316	1.2	0.373	2.8	0.898
B1 188.2 6.1	0.00	1648	1515	0.95	73.3	325.2	±7.9	318	±23	305.8	±8	–2	19.33	2.5	0.05275	1	19.33	2.5	0.05275	1	0.376	2.7	0.925
B1 188.2 7.1	–	2212	50	0.02	96.1	318.1	±7.7	330	±21	367	±24	4	19.78	2.5	0.05281	0.88	19.77	2.5	0.05304	0.92	0.3699	2.6	0.937
B1 188.2 8.1	–	1118	1138	1.05	47.6	311.8	±7.6	302	±32	304.2	±8.1	–3	20.19	2.5	0.05193	1.3	20.18	2.5	0.05238	1.4	0.358	2.9	0.868
B1 188.2 9.1	–	1404	1115	0.82	43.7	229.4	±5.6	372	±34	290.3	±7.8	62	27.61	2.5	0.0536	1.3	27.6	2.5	0.05402	1.5	0.2699	2.9	0.855
B1 188.2 10.1	–	983	468	0.49	45.2	336	±8.2	327	±30	336	±9.4	–3	18.7	2.5	0.05279	1.3	18.69	2.5	0.05295	1.3	0.391	2.8	0.885
B1 188.2 11.1	–	2116	163	0.08	91.2	315.7	±7.6	294	±21	334	±11	–7	19.93	2.5	0.05212	0.89	19.93	2.5	0.05219	0.9	0.3611	2.6	0.94
B1 188.2 12.1	0.07	1838	1750	0.98	78	310.8	±7.5	341	±25	306.5	±7.9	10	20.23	2.5	0.05382	0.96	20.25	2.5	0.05328	1.1	0.3628	2.7	0.915
B1 188.2 13.1	–	2374	3017	1.31	108	333.7	±8	351	±26	328.2	±8.7	5	18.83	2.5	0.05301	0.84	18.82	2.5	0.05353	1.1	0.392	2.7	0.907
B1 188.2 14.1	0.96	2206	2593	1.21	82.7	272.6	±6.6	383	±60	266.1	±7.3	41	22.93	2.5	0.062	0.9	23.15	2.5	0.0543	2.7	0.323	3.6	0.682
B1 188.2 15.1	0.09	882	1094	1.28	40.3	334.2	±8.2	341	±42	343.3	±9.3	2	18.78	2.5	0.05398	1.4	18.8	2.5	0.05329	1.8	0.391	3.1	0.806
B1 188.2 16.1	0.08	1907	1823	0.99	82.5	316.5	±7.6	319	±31	324.5	±8.5	1	19.85	2.5	0.05345	0.96	19.87	2.5	0.05278	1.4	0.366	2.8	0.878
B1 188.2 17.1	0.26	2099	185	0.09	93	323.4	±7.8	329	±34	350	±21	2	19.39	2.5	0.05513	0.89	19.44	2.5	0.05301	1.5	0.376	2.9	0.856
B1 188.2 18.1	0.00	2494	5046	2.09	117	343.1	±8.3	315	±19	332.1	±8.4	–8	18.29	2.5	0.05268	0.82	18.29	2.5	0.05268	0.82	0.397	2.6	0.949
B1 188.2 19.1	0.66	2390	1675	0.72	95.8	292	±7.1	377	±60	302.5	±9	29	21.44	2.5	0.05949	0.84	21.58	2.5	0.0542	2.7	0.346	3.6	0.682
B1 188.2 19.2	1.14	5807	5192	0.92	229	285.8	±6.9	479	±43	132.7	±4.5	68	21.81	2.5	0.06595	0.64	22.06	2.5	0.0567	2	0.354	3.2	0.784
B1 188.2 20.1	0.94	1479	1486	1.04	62.2	305.2	±7.4	307	±75	318.4	±9.2	1	20.43	2.5	0.06009	1	20.63	2.5	0.0525	3.3	0.351	4.1	0.604

Errors are 1σ; Pb_c and Pb* – the common and radiogenic portions, respectively; error in standard calibration was 0.86% (not included in above errors but required when comparing data from different mounts); (1) – common Pb corrected using measured ^{204}Pb

Table 4

SHRIMP data for zircons from the Bożnowice granodiorite, sample B1 117.5

Spot	$^{206}Pb_c$ [%]	U [ppm]	Th [ppm]	$^{232}Th/^{238}U$	^{206}Pb [ppm]*	(1) $^{206}Pb/^{238}U$ Age		(1) $^{207}Pb/^{206}Pb$ Age		(1) $^{208}Pb/^{232}Th$ Age		Discordant [%]	Total $^{238}U/^{206}Pb$	±%	Total $^{207}Pb/^{206}Pb$	±%	(1) $^{238}U/^{206}Pb^*$	±%	(1) $^{207}Pb^*/^{206}Pb^*$	±%	(1) $^{207}Pb^*/^{235}U$	±%	err-corr
B1 117.5 8.2	0.27	428	231	0.56	16.5	281.6	±6.7	348	±72	274.9	±9.6	24	22.33	2.4	0.0556	1.9	22.39	2.4	0.0535	3.2	0.329	4	0.608
B1 117.5 2.1	0.13	536	497	0.96	21.6	294.6	±7	286	±62	294.7	±8.3	–3	21.36	2.4	0.0531	2.1	21.39	2.4	0.052	2.7	0.335	3.7	0.669
B1 117.5 7.1	0.23	556	600	1.11	22.5	295.6	±7	308	±58	285.8	±7.9	4	21.26	2.4	0.05435	1.5	21.31	2.4	0.0525	2.5	0.34	3.5	0.687
B1 117.5 9.1	0.19	432	364	0.87	17.5	296.2	±7.1	311	±54	293.4	±8.4	5	21.22	2.4	0.05412	1.6	21.26	2.4	0.0526	2.4	0.341	3.4	0.717
B1 117.5 1.1	0.33	635	434	0.71	26.2	301.4	±7.3	236	±120	301.0	±12	–22	20.82	2.5	0.05353	1.8	20.89	2.5	0.0509	5.4	0.336	5.9	0.421
B1 117.5 9.2	0.23	895	866	1.00	37.1	303.1	±7.1	265	±63	298.8	±8.2	–13	20.72	2.4	0.05337	1.2	20.77	2.4	0.0515	2.7	0.342	3.6	0.66
B1 117.5 4.1	1.13	72	24	0.34	3.02	303.9	±8.5	352	±360	306.0	±62	16	20.48	2.7	0.0626	3.8	20.71	2.8	0.0535	16	0.356	16	0.177
B1 117.5 14.2	0.13	1030	590	0.59	42.8	304.5	±7.1	296	±51	300.1	±8.9	–3	20.65	2.4	0.05328	1.1	20.67	2.4	0.0522	2.3	0.348	3.3	0.729
B1 117.5 8.3	0.01	1410	672	0.49	58.7	304.9	±7.1	301	±21	289.1	±7.4	–1	20.64	2.4	0.05244	0.92	20.65	2.4	0.05236	0.93	0.3497	2.6	0.931
B1 117.5 12.2	0.1	1112	912	0.85	46.7	307.2	±7.2	305	±35	306.9	±7.9	–1	20.47	2.4	0.05323	0.99	20.49	2.4	0.05245	1.5	0.353	2.8	0.842
B1 117.5 8.1	0.3	199	88	0.46	8.38	307.4	±7.5	265	±120	309.0	±17	–14	20.41	2.5	0.054	2.4	20.47	2.5	0.0515	5.3	0.347	5.9	0.424
B1 117.5 10.2	0.04	974	659	0.7	40.9	307.6	±7.2	319	±29	305.0	±8.2	4	20.45	2.4	0.05309	1.1	20.46	2.4	0.05276	1.3	0.3556	2.7	0.884
B1 117.5 12.1	0.13	301	137	0.47	12.8	310.0	±7.4	317	±64	308.0	±11	2	20.27	2.4	0.0538	1.9	20.3	2.4	0.0527	2.8	0.358	3.7	0.657
B1 117.5 11.1	0.43	87	55	0.66	3.7	311.9	±8	304	±150	297.0	±17	–3	20.09	2.6	0.0559	3.5	20.18	2.6	0.0524	6.7	0.358	7.2	0.364
B1 117.5 3.1	0.2	841	563	0.69	35.9	312.2	±7.3	288	±57	310.6	±9.1	–8	20.11	2.4	0.05366	1.2	20.15	2.4	0.0521	2.5	0.356	3.5	0.691
B1 117.5 6.1	0.02	715	789	1.14	30.6	313.1	±7.4	338	±30	306.3	±7.9	8	20.09	2.4	0.05335	1.3	20.09	2.4	0.05321	1.3	0.365	2.7	0.877
B1 117.5 5.1	0.23	556	471	0.88	23.9	313.6	±7.4	270	±80	310.7	±9.6	–14	20.01	2.4	0.05354	1.4	20.06	2.4	0.0517	3.5	0.355	4.3	0.567
B1 117.5 4.2	0.07	1469	1148	0.81	63.0	313.8	±7.3	303	±25	311.9	±8.1	–3	20.04	2.4	0.053	0.88	20.05	2.4	0.05241	1.1	0.3604	2.6	0.907
B1 117.5 10.1	0.92	74	42	0.58	3.23	315.5	±8.5	135	±270	286.0	±26	–57	19.75	2.7	0.0561	4	19.93	2.7	0.0487	11	0.337	12	0.234
B1 117.5 13.2	0.07	1359	286	0.22	70.1	375.6	±8.7	429	±26	389.0	±12	14	16.66	2.4	0.056	0.82	16.67	2.4	0.05542	1.2	0.458	2.7	0.899
B1 117.5 13.1	0.16	1703	812	0.49	93.6	399.2	±9.2	545	±63	424.0	±13	37	15.63	2.4	0.0597	2.6	15.65	2.4	0.0584	2.9	0.514	3.7	0.639
B1 117.5 14.1	0.07	325	337	1.07	46.1	985.0	±22	974	±25	1026.0	±26	–1	6.05	2.4	0.0722	0.9	6.06	2.4	0.07159	1.2	1.629	2.7	0.889

Table 5

SHRIMP data for zircons from the Kalinka tonalite, sample KAL

Spot	$^{206}Pb_c$ [%]	U [ppm]	Th [ppm]	$^{232}Th/^{238}U$	$^{206}Pb^*$ [ppm]	(1) $^{206}Pb/^{238}U$ Age		(1) $^{207}Pb/^{206}Pb$ Age		Discordant [%]	Total $^{238}U/^{206}Pb$	±%	Total $^{207}Pb/^{206}Pb$	±%	(1) $^{238}U/^{206}Pb^*$	±%	(1) $^{207}Pb^*/^{206}Pb^*$	±%	(1) $^{207}Pb^*/^{235}U$	±%	err corr
KAL 1.1	0.09	365	366	1.04	14.9	299.1	±7.6	350	±57	17	21.04	2.6	0.0542	2.1	21.06	2.6	0.0535	2.5	0.35	3.6	0.721
KAL 2.1	0.4	312	316	1.05	12.2	285.9	±6.8	288	±120	1	21.96	2.4	0.0553	2.3	22.05	2.4	0.0521	5.4	0.325	5.9	0.412
KAL 3.1	0.06	683	1084	1.64	27.6	295.9	±6.8	279	±42	–6	21.28	2.4	0.05233	1.6	21.29	2.4	0.05186	1.8	0.336	3	0.792
KAL 4.1	0.00	692	1174	1.754	27.6	292.7	±6.8	343	±35	17	21.53	2.4	0.05336	1.6	21.53	2.4	0.05333	1.6	0.3415	2.8	0.834
KAL 5.1	0.04	365	223	0.63	14.5	292.3	±7	297	±52	2	21.55	2.4	0.0526	2.2	21.56	2.4	0.0523	2.3	0.334	3.3	0.73
KAL 6.1	0.33	404	81	0.21	16.3	295.1	±7	277	±120	–6	21.28	2.4	0.0544	2.1	21.34	2.4	0.0518	5.4	0.335	5.9	0.408
KAL 7.1	0.07	543	861	1.64	22.2	299.6	±6.9	302	±46	1	21.01	2.4	0.05291	1.7	21.02	2.4	0.0524	2	0.343	3.1	0.759
KAL 8.1	0.3	338	194	0.59	13.9	301.1	±7.1	262	±120	–13	20.85	2.4	0.0538	2.2	20.91	2.4	0.0515	5.1	0.339	5.7	0.426
KAL 8.2	1.26	96	50	0.53	3.87	290.4	±8.3	291	±460	0	21.42	2.6	0.0622	4.9	21.7	2.9	0.052	20	0.331	21	0.143
KAL 9.1	0.23	464	619	1.38	18.4	290.5	±6.8	247	±95	–15	21.64	2.4	0.05301	1.9	21.69	2.4	0.0511	4.1	0.325	4.8	0.501
KAL 10.1	0.69	272	135	0.52	11.1	296.7	±7.2	233	±190	–21	21.08	2.4	0.0564	2.4	21.23	2.5	0.0508	8.2	0.33	8.6	0.291
KAL 10.2	0.19	335	170	0.52	12.4	272.1	±6.4	296	±86	9	23.15	2.4	0.0538	2.3	23.19	2.4	0.0522	3.8	0.311	4.5	0.54
KAL 11.1	0.51	216	216	1.04	8.73	295	±7.2	242	±180	–18	21.24	2.4	0.0552	2.6	21.35	2.5	0.051	7.7	0.33	8.1	0.306
KAL 12.1	0.26	443	454	1.06	18.2	301.2	±7	268	±110	–11	20.85	2.4	0.0537	2.3	20.91	2.4	0.0516	4.7	0.34	5.3	0.455
KAL 13.1	0.29	388	478	1.27	16.9	317.9	±7.6	254	±120	–20	19.72	2.4	0.0536	2.5	19.78	2.4	0.0513	5.2	0.358	5.7	0.428
KAL 14.1	0.24	377	388	1.06	15.2	294.4	±6.9	313	±96	6	21.34	2.4	0.0546	2.1	21.4	2.4	0.0526	4.2	0.339	4.9	0.495
KAL 15.1	0.57	172	98	0.59	6.95	294.6	±8.3	265	±220	–10	21.26	2.8	0.0561	3.4	21.38	2.9	0.0515	9.6	0.332	10	0.288
KAL 16.1	0.05	1104	2232	2.09	44.2	293.4	±6.7	316	±32	8	21.47	2.3	0.0531	1.2	21.48	2.3	0.05271	1.4	0.3384	2.7	0.854
KAL 17.1	0.37	181	45	0.26	7.11	287.8	±7	293	±110	2	21.82	2.5	0.0551	3	21.9	2.5	0.0522	4.9	0.328	5.5	0.454
KAL 18.1	0.35	441	478	1.12	17.7	293	±7	277	±130	–6	21.43	2.4	0.0546	1.9	21.5	2.4	0.0518	5.7	0.332	6.2	0.393
KAL 19.1	0.3	519	606	1.21	21.5	302.4	±7.1	247	±97	–18	20.76	2.4	0.05351	1.8	20.82	2.4	0.0511	4.2	0.339	4.8	0.497
KAL 20.1	0.08	421	458	1.12	16.5	286.7	±6.7	319	±53	11	21.97	2.4	0.0534	2	21.99	2.4	0.0528	2.3	0.331	3.3	0.718

Errors are 1 σ; Pb_c and Pb* – the common and radiogenic portions, respectively; error in standard calibration was 0.74% (not included in above errors but required when comparing data from different mounts); (1) – common Pb corrected using measured ^{204}Pb

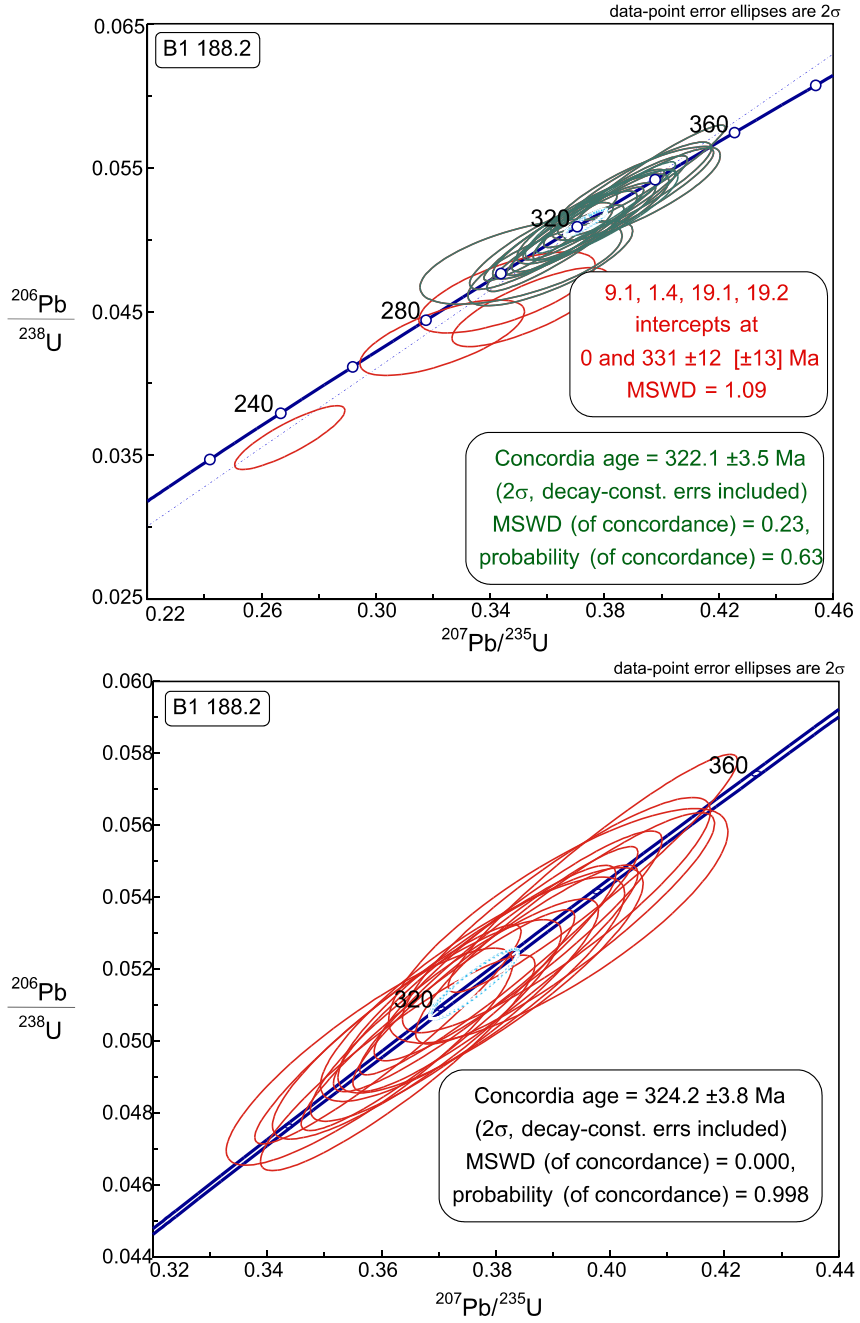

Fig. 9. Concordia diagram showing results of SHRIMP II zircon analyses from tonalite B1 188.2

presence of inheritance: zoned core 14.1 with a concordant age of 980 ±33 Ma, and positively discordant cloudy cores 13.1 of 545 ±63 Ma, and 13.2 of 429 ±26 Ma ($^{207}Pb/^{206}Pb$ minimum ages). These points, together with the main zircon population give intercepts at 947 ±66 Ma and 309 ±9 Ma.

The main age group of zircons are scattered between *ca*. 295 and 314 Ma, with an average Concordia age of 306 ±3 Ma (Fig. 11). An apparently younger point 8.2 is significantly positively discordant and thus its $^{207}Pb/^{206}Pb$ date of *ca*. 348 Ma may be assumed as a minimum age.

In conclusion, the main population of the zircons in this sample, displaying magmatic features (long- to normal prismatic habit, oscillatory zonation, high Th/U ratios), are dated at 306 ±3 Ma. Rather scarce inheritance is *ca*. 1.0 Ga old and seems to be partly reset by the younger magmatic event.

KALINKA TONALITE, SAMPLE KAL

All zircon grains from this tonalite are also alike: long-prismatic, pencil-like, with steep or flat pyramids (Fig. 12). Many crystals are broken. Also many display characteristic zoning in CL images, with alternating bright and dark bands aligned with the length of the crystals, with no clear bands parallel to the pyramids. CL-dark vacuoles are common, and no distinct cores are observable.

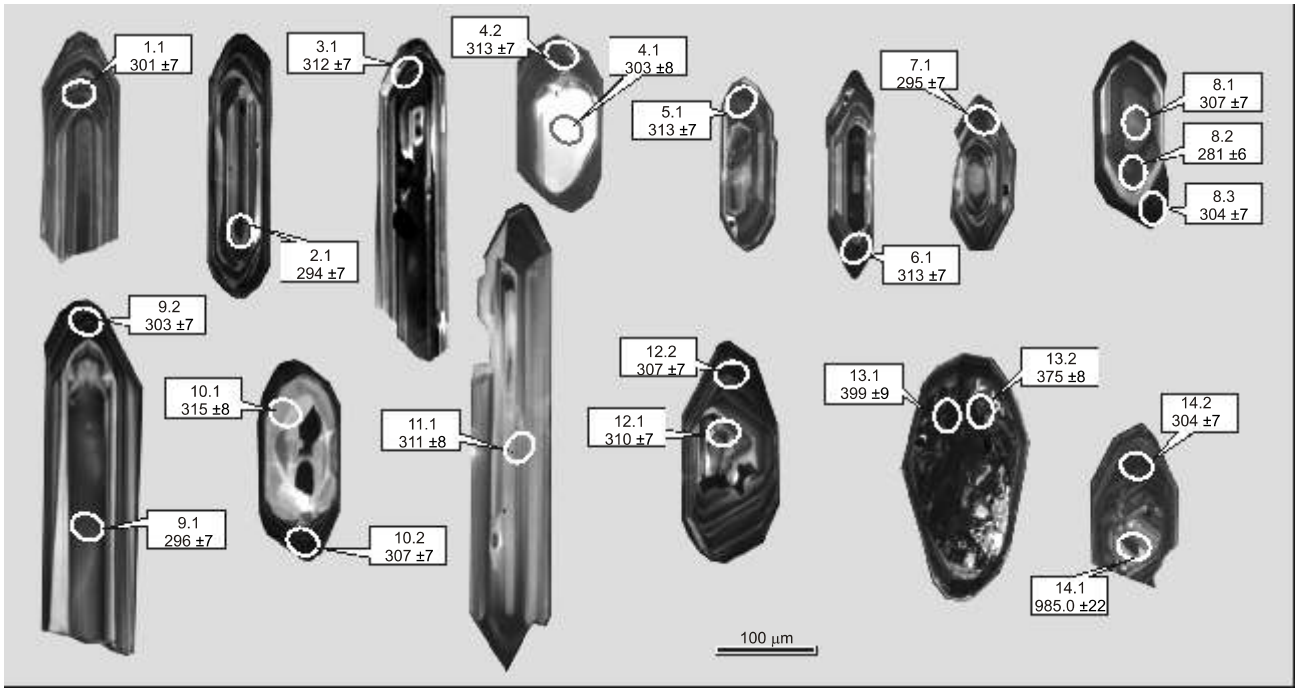

Fig. 10. Cathodoluminescence images of zircons analysed from granodiorite B1 117.5

Symbols of analytical points correspond to those in Table 4; $^{206}Pb/^{238}U$ ages and one σ errors are given

Among the 22 points analysed, no distinctly older inherited grains were found, though three of the spots, with significant positive discordance, may have $^{207}Pb/^{206}Pb$ ages approximating their minimum ages: point 20.1 = *ca*. 319 Ma, point 4.1 = *ca*. 343 Ma, and point 1.1 = *ca*. 350 Ma (Table 5).

The remaining 19 points are concordant or only slightly discordant, with a few grains with rather significant negative discordance D, up to –21. The mean Concordia age for all 22 points is 294 ±3 Ma (Fig. 13). Taking into account the observed homogeneity of the zircon population in this sample and their magmatic features, this Concordia age can be interpreted as a good approximation of the true magmatic age of the Kalinka tonalite.

DISCUSSION

SEQUENCE AND P-T CONDITIONS OF THE THERMAL EVENTS

The tectono-metamorphic history of the eastern part of the Strzelin Massif was studied by Wojnar (1995), Oberc-Dziedzic and Szczepański (1995), Oberc-Dziedzic (1999), Szczepański and Józefiak (1999), Szczepański (2001), Oberc-Dziedzic and Madej (2002). A summary of their results is presented below.

The Strzelin and Nowolesie gneisses contain two groups of zircons dated at ~600–568 Ma by U/Pb SHRIMP analyses (Oberc-Dziedzic *et al.*, 2003*a*; Klimas, 2008). The younger group of zircon ages (568 Ma) is taken as a record of late Proterozoic crystallization during partial melting associated with metamorphism which affected the *ca*. 600 Ma protolith of the Strzelin gneiss (Oberc-Dziedzic *et al.*, 2003*a*). However, the pre-Devonian deformation and metamorphism of the gneisses and of the older schist series in the Strzelin Massif have not been proved (Wojnar, 1995). The tectonic structures, their sequence and metamorphic conditions are common for the Neoproterozoic gneisses, older schist series and Devonian Jegłowa Beds and are considered as Variscan. Unlike the Strzelin Massif, Neoproterozoic structures were identified in paragneisses of the northern part of the Desna Dome in Silesicum (Żelaźniewicz *et al.*, 2005). These structures are older than a metapegmatite vein containing zircons dated at ~580 Ma (U-Pb SHRIMP method) which cross-cuts amphibolite facies paragneisses (Żelaźniewicz *et al.*, 2005). The lack of Neoproterozoic structures in the rocks of the Strzelin Massif and the presence of such structures in the paragneisses of the Desna Dome may mean that the Proterozoic rocks of these two units belong to separate blocks of Brunovistulicum basement characterized by different tectonic histories.

All three groups of rocks in the Strzelin Massif: the gneisses, older schist series, and Jegłowa Beds, show evidence of four metamorphic events (Oberc-Dziedzic, 1999). The effects of the M_1–M_3 metamorphic episodes are different in the northern and southern parts of the massif, implying that both parts have derived from various metamorphic zones (Szczepański, 2001; Oberc-Dziedzic and Madej, 2002). In both parts, the M_1 metamorphic episode was coeval with the D_1 deformation and nappe stacking during the collision of Moldanubicum with Brunovistulicum. The M_2 episode took place during and after D_2, and involved a temperature increase under constant pressure (Oberc-Dziedzic, 1999).

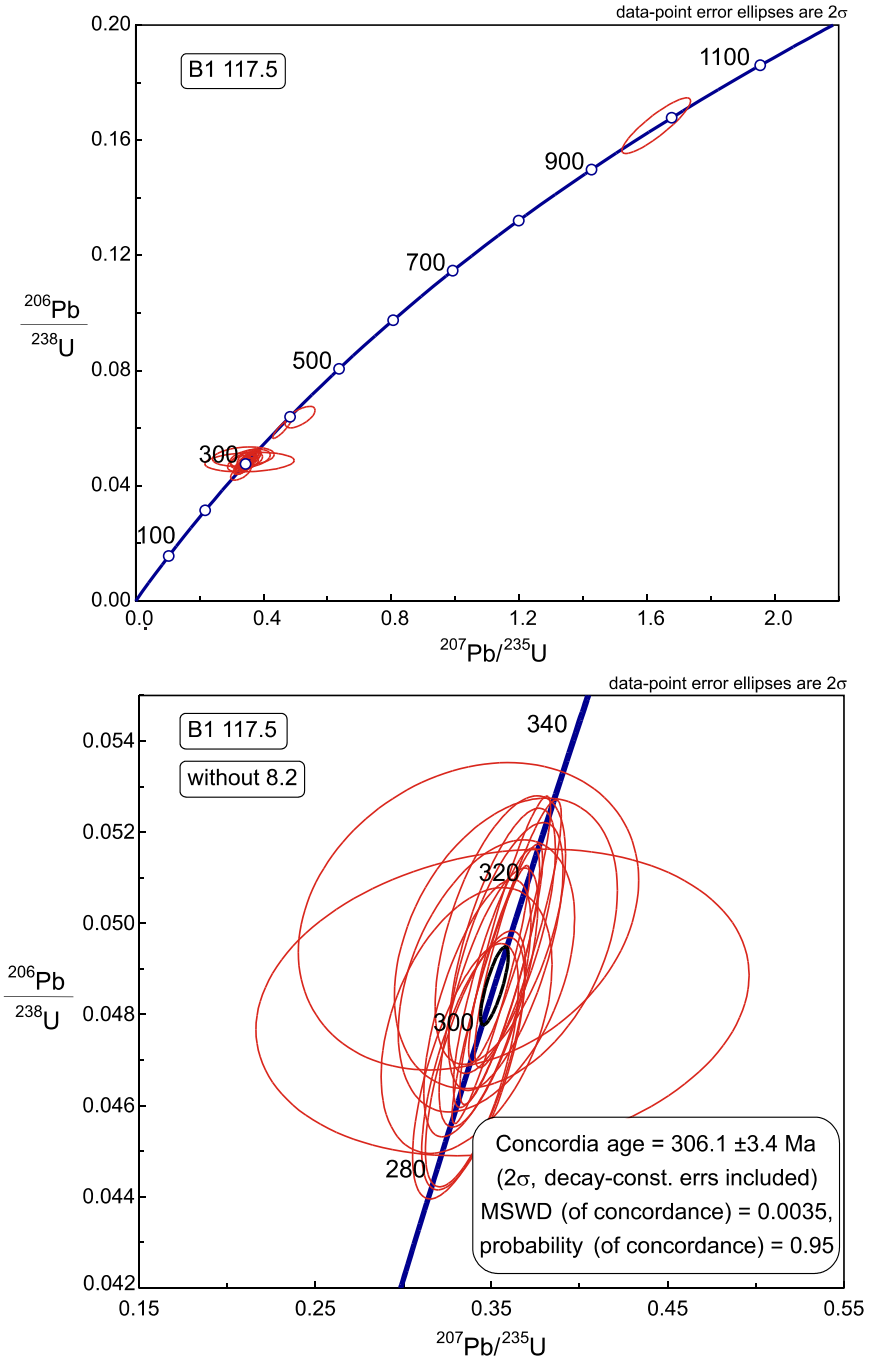

Fig. 11. Concordia diagram showing results of SHRIMP II zircon analyses from granodiorite B1 117.5

In the northern domain of the massif, metamorphic conditions during metamorphic event M_1 were typical of greenschist facies in the case of the Jegłowa Beds, and of amphibolite facies in the case of the Strzelin gneiss. The rocks of the older schist series bear a record of continuous transition from greenschist facies to amphibolite facies conditions (Oberc-Dziedzic, 1999). The temperature during the M_2 metamorphic event was probably similar to that of M_1. The M_3 metamorphic episode, which was coeval with the D_3 and D_4 deformation events, took place under lower amphibolite-greenschist facies conditions and caused local retrogressive changes.

In the southern part of the Strzelin Massif, the nappe stacking gave rise to crustal thickening and increase in temperature, and caused the gneisses to achieve anatectic conditions, estimated as 720–730°C and 6.5–5 kb (Oberc-Dziedzic, 1999). The thin leucosome layers formed during the first stage of migmatization were parallel to the S_1 foliation. They were folded into the F_2 folds during the D_2 deformation. Subsequently, sillimanite nodules parallel to the axial plane cleavage of the F_2 folds (sillimanite I) were formed (Wojnar, 1995; Oberc-Dziedzic and Madej, 2002). After D_2, the second anatexis stage took place. This M_2 metamorphic event proceeded with no deformation, giving rise to the formation of

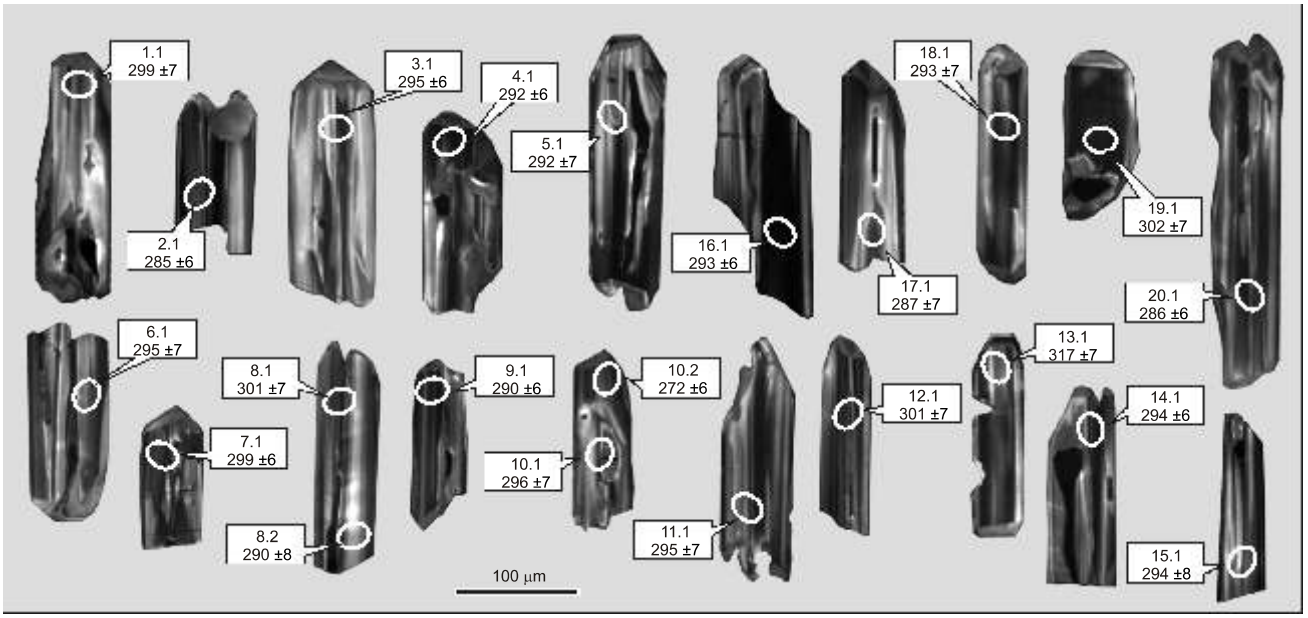

Fig. 12. Cathodoluminescence images of zircons analysed from tonalite KAL

Symbols of analytical points correspond to those in Table 5; $^{206}Pb/^{238}U$ ages and one σ errors are given

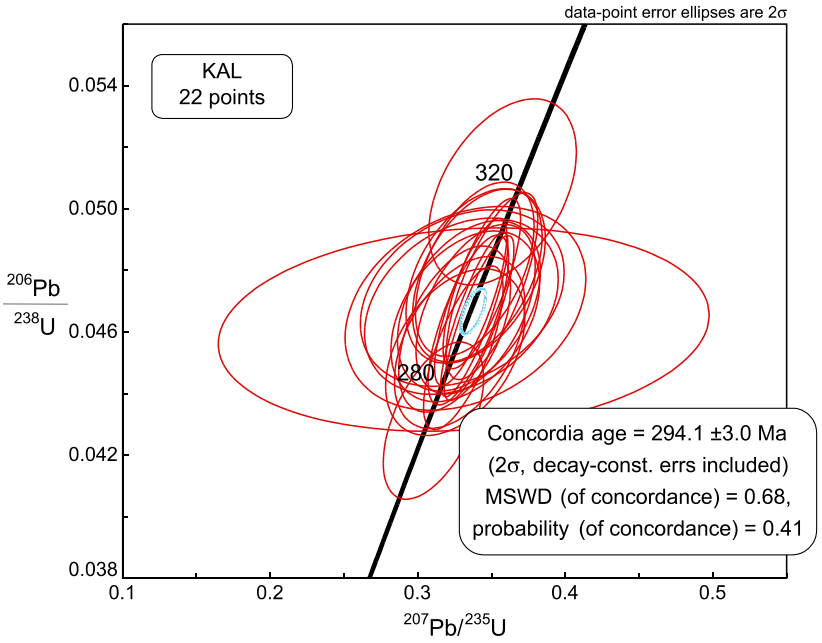

Fig. 13. Concordia diagram showing results of SHRIMP II zircon analyses from tonalite KAL

pegmatites and leucocratic granites. The P-T conditions of M_2 were estimated in the pegmatites at T = 600° and P = 3 kb (Oberc-Dziedzic, 1999). The M_3 metamorphic event was coeval with the D_3 deformation and probably took place under conditions similar to those of M_2, since the deformed sillimanite nodules show no retrogression reactions. During M_3, elongated quartz grains with sillimanite inclusions were formed in the gneisses, and sillimanite II appeared in the slightly deformed pegmatites (Oberc-Dziedzic, 1999).

The final metamorphic episode M_4 led to the crystallization of postkinematic cordierite and the formation of flecky gneisses. The crystallization of cordierite took place under P-T conditions in which sillimanite and garnet were stable. The cordierite was formed after the migmatization and before the emplacement of the granites and tonalites (Oberc-Dziedzic, 1995).

AGE OF METAMORPHIC AND MAGMATIC EVENTS

The Strzelin orthogneiss, typical of the northern part of the Strzelin Massif, was dated at 600 ±7 and 568 ±7 Ma (SHRIMP U/Pb zircon age; Oberc-Dziedzic *et al*., 2003*a*). Similar mean zircon ages (602 ±7 and 587 ±4 Ma, Klimas, 2008; 576–560 Ma, Mazur *et al*., 2010) were obtained for the Nowolesie gneiss from the southern part of the massif. These Cadomian ages of the gneisses of the Strzelin Massif are similar to the ages of basement rocks of the Keprník and Desna domes (Oberc-Dziedzic *et al*., 2003*a*), exposed in Silesicum (Jeseník Mountains), which represent the marginal, imbricated part of Brunovistulicum (Schulmann and Gayer, 2000). Although isotopic data reflecting the metamorphic events during the Variscan D_1 and D_2 compressive deformation have yet not been reported from the study area, it is likely that the metamorphism began after the collision of Moldanubicum with Brunovistulicum, i.e. about 330–335 Ma (Schulmann *et al*., 2009). In the Strzelin Massif, the metamorphic imprint connected with extensional D_3 and D_4 deformation events was weak and restricted to narrow mylonitic zones (Oberc-Dziedzic, 1999). The age of the extensional deformation in this area remains unknown. In the Keprník and Desna domes, the $^{40}Ar/^{39}Ar$ radiometric age of 300–310 Ma has been interpreted as linked with the extensional process during the Westphalian (Maluski *et al*., 1995). The tectono-metamorphic imprint in the Keprník area around 305 Ma was strong enough to completely reset the mineral assembalges (Maluski *et al*., 1995).

The U/Pb SHRIMP zircon ages of the granodiorite and two tonalites from the Strzelin Massif presented here in this paper, reveal three distinct stages of the Variscan magmatism: tonalitic I – at 324 Ma, granodioritic – at 305 Ma, and tonalitic II – at 295 Ma.

The structural relationships between the country rocks and the Bożnowice tonalite (sample B1 188.2) suggest that the first stage of magmatism, represented by the 324 Ma tonalite, took place after the regional metamorphism and anatectic migmatization connected with thickening, during the collision of Brunovistulicum with the Moldanubian Zone.

The second, granodioritic stage at 305 Ma took place when the migmatization ceased and the extensional conditions (D_3 deformation) began. This is supported by some common features of the migmatized gneisses and granodiorite as well as the fact that granodiorite bodies cross-cut the migmatized gneisses. The U/Pb zircon age of the granodiorite (sample B1 117.5) is in agreement with the biotite $^{40}Ar/^{39}Ar$ radiometric age of 304.4 ±3.1 Ma, obtained for the extensional conditions in the Keprník Dome (Maluski *et al*., 1995). The position of the Bożnowice granodiorite in the thermal evolution of the Strzelin Massif is similar to the position of pegmatites connected with the second stage of the migmatization which occurred after the D_2 metamorphic event and is recorded in the Nowolesie gneiss (Oberc-Dziedzic, 1999).

The third stage of the Variscan magmatism at ~295 Ma, represented by the Kalinka tonalite, corresponds to the late stage of thermal evolution of the Strzelin Massif. A similar age was also established for the Gęsiniec tonalite in the northern part of the massif (Pietranik and Waight, 2005) and for biotite granites (Turniak *et al*., 2006). The usually sharp and discordant contacts of all the ~295 Ma tonalites and granites with their country rocks and the presence of distinct chilled zones of these intrusions (Oberc-Dziedzic, 1991) suggest that the tonalite and biotite granite magmas intruded into relatively cool rocks.

The K/Ar age of the Strzelin biotite granite, varying between 278–288 Ma and previously interpreted as the age of the magma crystallization (Depciuch and Lis, 1972), probably corresponds to the cooling age of the granitoids. This age is similar to the Ar-Ar results of 279–285 Ma obtained for white micas from the Jegłowa Beds and interpreted as cooling ages related to the exhumation of the Strzelin Massif and corresponding to passing the isotherms of 330–430°C (Szczepański, 2002).

ORIGIN AND CRYSTALLIZATION OF GRANITOID MAGMAS

GRANODIORITE

The granodiorite studied is undoubtedly an igneous rock showing such features as intrusive contacts, structures typical of crystallization from melt, and chemical influence on its neighborhood, as shown by large grains of plagioclase in the surrounding migmatite. However, some other characteristics, such as: rounded shape of mineral grains, linear arrangement of K-feldspar, schlieren, all resemble features of highly evolved migmatites:diatexites (Mehnert, 1968).

A magmatic origin of the granodiorite is supported by the strong oscillatory zonation of zircon grains. The ages of a few inherited zircon cores (980 ±33 Ma and 545 ±63 Ma), fairly similar to the ages reported from gneisses of the area (Oberc-Dziedzic *et al*., 2003*a*; Klimas, 2008), suggest that the gneisses could have been the source material for the granodiorite magma. The crustal origin of the granodiorite magma is also suggested by the peraluminous character of the rock, its Zr/Nb, Nb/Th and Ce/Pb ratios, characteristic of continental crust. However, the multi-element diagram of trace element concentrations normalized to chondrite does not show negative anomalies of Nb and Ta, usually considered as typical of continental crust material (Taylor and McLennan, 1985). Moreover, the Bożnowice granodiorite is very rich in Ba and Sr, that is typical of mantle related, mafic magma (Słaby *et al*., 2008, and references therein).

The contradictory features mentioned above indicate a possible mixed crustal-mantle origin of the granodiorite magma. This seems to be supported by the value of the $\varepsilon Nd = -7.7$, considerably higher than $\varepsilon Nd = -10$ to -12 of the gneisses from the Strzelin Massif (Oberc-Dziedzic *et al*., 2009*b*), suggesting a more mafic source for the granodiorite. This does not necessarily mean a real input of the mantle magma but rather of material coming from mafic components of the lower crust (amphibolites or gabbros), or mantle-derived fluids.

The "anatectic" features of the Bożnowice granodiorite suggest that the magma was emplaced and crystallized not far from the place of its origin. The nearly identical size, composition and structure of large plagioclase crystals in the granodiorite and in the adjacent migmatite indicate that the large plagioclase in the migmatite crystallized from the

granodiorite-magma derived fluids. The crystallization of the large plagioclase in both the granodiorite and migmatite probably took place at the same time, i.e. after the magma emplacement.

The crystallization of large plagioclase and K-feldspar grains was two-phased but probably not coeval. During the first phase, plagioclase cores containing ~40–46% An, and Ba-poor euhedral grains of K-feldspar were formed. After that, the crystallization of both feldspars was interrupted: the plagioclase cores were subjected to corrosion, and thin zone of inclusions composed of $Or_{56.7}$-$Ab_{31.6}$-$An_{10.7}$-$Cs_{1.0}$ feldspar (former melt?) came into existence along the borders of the inner parts of K-feldspar grains. During the second phase of crystallization, the rims were formed around the feldspars cores. The characteristic features of the rims are oscillatory changes: 35–26–30% An contents in the rims of rounded plagioclase grains, and zonal enrichment in Ba of the subhedral rims of K-feldspar crystals. The crystallization of matrix minerals: biotite, small, rounded An_{28} plagioclase, quartz and interstitial, anhedral K-feldspar started at the end of the second phase of crystallization of large grains of K-feldspar and plagioclase.

TONALITES

The most important difference of the two tonalites studied are their ages: ~324 Ma for the Bożnowice tonalite and 295 Ma for the Kalinka tonalite. In spite of such a large age difference, their other features are generally similar. Both the tonalites show small differences in major element contents. The Bożnowice tonalite contains about 2.5% more SiO_2 and about 0.6% more MgO but less TiO_2, Al_2O_3, Fe_2O_3 and Na_2O than the Kalinka tonalite. These differences are mirrored in the biotite, amphibole and plagioclase compositions. Interestingly, the abundances of particular trace elements, apart from higher contents of Ni, Cu and U in the Bożnowice tonalite, as well as REE contents, the Eu anomaly and εNd values are similar in both tonalites. The εNd values of –4.0 to –4.3 are outside the range of typical mantle compositions and indicate a likely crustal source of the magma, with possible mantle-derived admixture.

The Bożnowice and Kalinka tonalites show some differences in grain-size and texture: the Bożnowice tonalite is medium-grained, the Kalinka tonalite is fine-grained. A important feature of the Bożnowice tonalite is plagioclase clusters surrounded by a common rim. The larger grains of plagioclase from the Bożnowice tonalite display a dismembered, embayed core, containing up to 76% An, surrounded by euhedral inner part composed of 38–42% An plagioclase, and by irregular, zoned rims (outer part) in which the An content decreases from 64 to 32%. Similar dismembered plagioclase cores from the Gęsiniec tonalite in the northern part of the Strzelin Massif (Fig. 2), were interpreted by Pietranik and Waight (2008) as an effect of the resorption due to decompression during the emplacement of phenocryst-bearing magmas in the upper crust. The simple structure of plagioclases such as in the Kalinka tonalite could be attributed to open-system processes in the lower crust (Pietranik and Waight, 2008).

As mentioned above, the magma of the Bożnowice tonalite crystallized soon after the beginning of the Variscan thermal events. It means that the ~324 Ma tonalite remained at relatively high temperatures for about 30 Ma.

CONCLUSION

The western margin of Brunovistulicum is characterized by an increase of thermal and magmatic activities during the Variscan orogeny from the southern, Moravian part, devoid of Variscan plutons, through the middle, Silesian part, with its Žulova Pluton, to the northern part, in the Strzelin Massif, where the basement rocks achieved anatectic conditions and Variscan granitoids form a range of small intrusions of various ages and compositions.

The U/Pb SHRIMP ages revealed three distinct stages of Carboniferous–early Permian magmatism in the southern part of the Strzelin Massif: tonalitic – at 324 Ma, granodioritic – at 305 Ma, and tonalitic/granitic – at 295 Ma; the biotite- and biotite-muscovite granites, most widespread in the entire Strzelin Masiif, have not been considered in detail in this paper. The first, discrete stage of magmatism took place after the regional metamorphism and anatectic migmatization connected with crustal thickening during the collision of Brunovistulicum with the Moldanubian Zone. The second stage of magmatism was coeval with the second stage of migmatization, which produced abundant pegmatites. This was related to decompression at the beginning of tectonic denudation. The third, most intense stage of magmatism was connected with the late thermal stage in the Strzelin Massif.

The Bożnowice granodiorite magma was emplaced and crystallized not far from the place of its origin. The source of that magma could have been the Neoproterozoic material of the lower crust.

The tonalites of ~324 Ma and 295 Ma are generally geochemically similar, in spite of their large age difference. The values of εNd of –4.0 to –4.3 are outside the range of typical mantle compositions and indicate a likely crustal source of magma, with possible mantle-derived admixture.

Acknowledgements. This research was carried out under the Project 2PO4D 028 27 of the Ministry of Science and Information. C. Pin is thanked for performing the Sm-Nd isotope analyses within the Research Project N307 008 32/0314 of the Polish Ministry of Science and Education. F. Finger and A. Żelaźniewicz are thanked for their constructive reviews. The authors are indebted also to Dr. P. Dzierżanowski and Ms. L. Jeżak, both from the University of Warsaw, for their kind assistance in carrying out the microprobe analyses.

REFERENCES

ALEKSANDROWSKI P. and MAZUR S. (2002) – Collage tectonics in the northeasternmost part of the Variscan Belt: the Sudetes, Bohemian Massif. In: Palaeozoic Amalgamation of Central Europe (eds. J. A. Winchester, T. C. Pharaoh and J. Verniers). Geol. Soc., Lond., Spec. Publ., **201**: 237–277.

BADURA J. (1979) – Szczegółowa mapa geologiczna Sudetów. Arkusz Stolec 1:25 000. Wyd. Geol., Inst. Geol.

BEDERKE E. (1931) – Die moldanubische Überschiebung im Sudetenvorlände. Zentralblatt für Mineral. Geol. Paläont. Abt. B: 349–408.

BEREŚ B. (1969) – Petrography of granite of the environments of Strzelin. (in Polish with English summary). Arch. Miner., **28**: 5–105.

BIAŁEK J. (2006) – Kalinka tonalites – petrography and geochemical characteristic (Strzelin Crystalline Massif, SW Poland). Miner. Pol., Spec. Pap., **29**: 95–98.

BLACK L. P., KAMO S. L., ALLEN C. M., ALEINIKOFF J. N., DAVIS D. W., KORSCH R. J. and FOUDOULIS C. (2003) – TEMORA 1: a new zircon standard for Phanerozoic U–Pb geochronology. Chem. Geol., **200**: 155–170.

CHÁB J., FIŠERA M., FEDIUKOVÁ E., NOVOTNY P., OPLETAL M. and SKÁCELOVÁ D. (1984) – Problems of the tectonic and metamorphic evolution of the eastern part of the Hrubý Jeseník Mts. (Altfatergebirge), northern Moravia, Czechoslovakia (in Czech with English summary). Sbor. Geol. Věd, Geol., **39**: 27–72.

CHÁB J., MIXA P., VAN-ČEK M. and ŽAČEK V. (1994*a*) – Geology of the NW part of the Hrubý Jeseník Mts. (the Bohemian massif, Central Europe). Věstník Českého geologického ústavu, **69** (3): 17–26.

CHÁB J. and ŽAČEK V. (1994) – Geology of the Žulová pluton mantle (Bohemian Massif, Central Europe). Věstník Českého geologického ústavu, **69** (4): 1–12.

CHLUPÁČ I. (1975) – New finds of fauna in the metamorphic Devonian of the Hruby Jeseník Mts. (Moravia, Czechoslovakia) (in Czech with English summary). Čas. Miner. Geol., **20**: 259–268.

CYMERMAN Z. (1993) – Tectonic units of the Strzelin metamorphic complex (Lower Silesia, SW Poland) in light of a new structural analysis (in Polish with English summary). Prz. Geol., **41** (6): 421–427.

CYMERMAN Z. and PIASECKI M. A. J. (1994) – The terrane concept in the Sudetes, Bohemian Massif. Geol. Quart., **38** (2): 191–210.

CYMERMAN Z., PIASECKI M. A. J. and SESTON R. (1997) – Terranes and terrane boundaries in the Sudetes, northeast Bohemian Massif. Geol. Mag., **134**: 717–725.

De PAOLO D. J. (1981*a*) – Neodymium isotopes in the Colorado Front Range and crust – mantle evolution in the Proterozoic. Nature, **291**: 193–196.

De PAOLO D. J. (1981*b*) – A Nd and Sr isotopic study of Mesozoic calc-alkaline batholiths of the Sierra Nevada and Peninsular Ranges, California. J. Geoph. Res., **86**: 10370–10488.

DEPCIUCH T. and LIS J. (1972) – Absolute age of K-Ar granitoids from Strzelin (Lower Silesia) (in Polish with English summary). Kwart. Geol., **16**: 95–102.

DUDEK A. (1980) – The crystalline basement block of the outer Carpathians in Moravia-Bruno-Vistulicum. Rozpravy Československé Akademie Véd, Řada matematických a přirodnich Véd, **90**: 1–85.

FINGER F., FRASL G., HÖCK V. and STEYRER H. P. (1989) – The granitoids of the Moravian Zone of north-east Austria – products of a Cadomian active continental margin? Precambr. Research, **45**: 235–245.

FINGER F., HANŽL P., PIN C., Von QUADT A. and STEYRER H. P. (2000) – The Brunovistulian: Avalonian Precambrian sequence at the eastern end of the Central European Variscides? (eds. W. Franke, V. Haak, O. Oncken and D. Tanner). Geol. Soc., Lond., Spec. Publ., **179**: 103–112.

FRANKE W. (1989) – Tectonostratigraphic units in the Variscan belt of Central Europe. Geol. Soc. Am. Spec. Pap., **230**: 67–89.

FRANKE W. (2000) – The mid-European segment of the Variscides: tectonostratigraphic units, terrane boundaries and plate tectonic evolution. In: Orogenic Processes: Quantification and Modelling in the Variscan Belt (eds. W. Franke, V. Haak, O. Oncken and D. Tanner). Geol. Soc., Lond., Spec. Publ., **179**: 35–61.

FRANKE W. and ŻELAŹNIEWICZ A. (2000) – The eastern termination of the Variscides: terrane correlation and kinematic evolution. In: Orogenic Processes: Quantification and Modelling in the Variscan Belt (eds. W. Franke, V. Haak, O. Oncken and D. Tanner). Geol. Soc., Lond., Spec. Publ., **179**: 63–86.

FRANKE W. and ŻELAŹNIEWICZ A. (2002) – Structure and evolution of the Bohemian Arc. In: Palaeozoic Amalgamation of Central Europe (eds. J. A. Winchester, T. C. Pharaoh and J. Verniers). Geol. Soc., Lond., Spec. Publ., **201**: 279–293.

FRANKE W., ŻELAŹNIEWICZ A., PORĘBSKI S. J. and WAJSPRYCH B. (1993) – Saxothuringian zone in Germany and Poland: differences and common features. Geol. Rundsch., **82**: 583–599.

FRIEDL G., FINGER F., MCNAUGHTON N. J. and FLETCHER J. R. (2000) – Deducing the ancestry of terranes: SHRIMP evidence for South America – derived Gondwana fragments in central Europe. Geology, **28**: 1035–1038.

GREEN T. H. (1980) – Island arc and continent-building magmatism – a review of petrogenetic models based on experimental petrology and geochemistry. Tectonophysics, **63**: 367–385.

HANSON G. H. (1978) – The application of trace elements to the petrogenesis of igneous rocks of granitic composition. Earth Planet. Sc. Lett., **38**: 26–41.

HASKIN L. A., HASKIN M. A., FREY F. A. and WILDMAN T. R. (1968) – Relative and absolute terrestrial abundances of the rare earths. In: Origin and Distribution of the Elements (eds. L. H. Ahrens). Pergamon Oxford, **1**: 889–911.

HOFMANN A. W. (1988) – Chemical differentiation of the Earth: the relationship between mantle, continental crust, and oceanic crust. Earth Planet. Sc. Lett., **80**: 297–314.

KLIMAS K. (2008) – Geochronology and petrogenetical study of zircons from selected crystalline rocks in the eastern part of the Fore-Sudetic Block (in Polish with English summary). Uniwersytet Wrocławski, Inst. Nauk Geol., Wrocław.

KOSSMAT F. (1927) – Gliederung des varistischen Gebirgsbaues. Abhandlungen Sächsischen Geologischen Landesamts, **1**: 1–39.

KRÖNER A., JAECKEL P., HEGNER E. and OPLETAL M. (2001) – Single zircon ages and whole-rock Nd isotopic systematics of early Palaeozoic granitoid gneisses from the Czech and Polish Sudetes (Jizerské hory, Krkonoše Mountains and Orlice-Sniežník Complex). Int. J. Earth Sc., **90**: 304–324.

KRÖNER A. and MAZUR S. (2003) – Proterozoic and Palaeozoic crustal components across the East/Central Sudetes boundary at the eastern margin of the Bohemian Massif: new U/Pb single zircon ages from the eastern Fore-Sudetic block (SW Poland). J. Czech Geol. Soc. Abstract Volume, **48** (1–2): 83–84.

KRÖNER A., ŠTÍPSKÁ P., SCHULMANN K. and JAECKEL P. (2000) – Chronological constraints on the pre-Variscan evolution of the northeastern margin of the Bohemian Massif, Czech Republic. In: Orogenic Processes: Quantification and Modelling in the Variscan Belt (eds. W. Franke, V. Haak, O. Oncken and D. Tanner). Geol. Soc. Lond., Spec. Publ., **179**: 175–197.

LARIONOV A. N., ANDREICHEV V. A. and GEE D. G. (2004) – The Vendian alkaline igneous suite of northern Timan: on microprobe U–Pb zircon ages of gabbros and syenite. In: The Neoproterozoic Timanide Orogen of Eastern Baltica (eds. D. G. Gee and V. L. Pease). Geol. Soc. London Mem., **30**: 69–74.

LEAKE B., WOOLEY A. R., ARPS C. E. S. and BIRCH W. D. *et al*. (1997) – Nomenclature of amphiboles: report of the Subcommittee on Amphiboles of the International Mineralogical Association, Commission on New Minerals and Mineral Names. Can. Miner., **35**: 219–246.

LORENC M. W. (1987) – Cordierite in granitoid rocks of Hercynian massifs of the Central System (Estremadura, Spain) – a preliminary comparative study (in Polish with English summary). Ann. Soc. Geol. Pol., **57**: 89–106.

LUDWIG K. R. (2005*a*) – SQUID 1.12 A User's Manual. A Geochronological Toolkit for Microsoft Excel. Berkeley Geochronology Center Special Publication: 1–22, http://www.bgc.org/klprogrammenu.html

LUDWIG K. R. (2005*b*) – User's Manual for ISOPLOT/Ex 3.22. A Geochronological Toolkit for Microsoft Excel. Berkeley Geochronology Center Special Publication: 1–71, http://www.bgc.org/klprogrammenu.html

MALUSKI H., RAJLICH P. and SOUČEK J. (1995) – Pre-variscan, Variscan and Early Alpine thermo-tectonic history of the north-eastern Bohemian Massif: An $^{40}Ar/^{39}Ar$ study. Geol Rundsch., **84**: 345–358.

MATTE P., MALUSKI H., RAJLICH P. and FRANKE W. (1990) – Terrane boundaries in the Bohemian Massif: results of large scale Variscan shearing. Tectonophysics, **177**: 151–170.

MAZUR S., ALEKSANDROWSKI P., KRYZA R. and OBERC-DZIEDZIC T. (2006) – The Variscan Orogen in Poland. Geol. Quart., **50** (1): 89–118.

MAZUR S., KRÖNER A., SZCZEPAŃSKI J., TURNIAK K., HANŽL P., MELICHAR R., RODIONOV N. V., PADERIN I. and SERGEEV S. A. (2010) – Single zircon U-Pb ages and geochemistry of granitoid gneisses from SW Poland: evidence for an Avalonian affinity of the Brunian microcontinent. Geol. Mag., **147** (4): 508–526.

McLENNAN S. M., TAYLOR S. R. and HEMMING S. R. (2006) – Composition, differentiation, and evolution of continental crust: constraints from sedimentary rocks and heat flow. In: Evolution and Differentiation of the Continental Crust (eds. M. Brown and T. Rushmer): 92–134. Cambridge University Press.

MEHNERT K. R. (1968) – Migmatites and the origin of granitic rocks. Elsevier Publishing Company, Amsterdam, London, New York.

NAKAMURA N. (1974) – Determination of REE, Ba, Fe, Mg, Na and K in carbonaceous and ordinary chondrites. Geoch. Cosmoch. Acta, **38**: 757–775.

NUTMAN A. P., BENNET V. C., FRIEND C. R. L. and NORMAN M. D. (1999) – Meta-igneous (non-gneissic) tonalites and quartz-diorites from an extensive *ca*. 3800 Ma terrain south of the Isua supracrustal belt, southern West Greenland: constraints on early crust formation. Contrib. Miner. Petrol., **137**: 364–388.

OBERC J. (1966) – Geology of crystalline rocks of the Wzgórza Strzelińskie Hills, Lower Silesia (in Polish with English summary). Stud. Geol. Pol., **20**: 1–187.

OBERC J., OBERC-DZIEDZIC T. and KLIMAS-AUGUST K. (1988) – Mapa geologiczna Wzgórz Strzelińskich w skali 1:25 000 (ed. J. Oberc). Inst. Nauk Geol. Uniw. Wrocławskiego, Przedsiębiorstwo Geologiczne Wrocław.

OBERC-DZIEDZIC T. (1991) – Geological setting of the Strzelin granitoids (in Polish with English summary). Acta Univ. Wratisl., 1375. Pr. Geol.-Miner., **29**: 295–324.

OBERC-DZIEDZIC T. (1995) – Research problems of the Wzgórza Strzelińskie metamorphic series in the light of the analysis of borehole materials (in Polish with English summary). Acta Univ. Wratisl., 1739, Pr. Geol.-Miner., **50**: 75–105.

OBERC-DZIEDZIC T. (1999) – The metamorphic and structural development of gneisses and older schist series in the Strzelin Crystalline Massif (Fore-Sudetic Block, SW Poland). Miner. Soc. Pol. Spec. Pap., **14**: 10–21.

OBERC-DZIEDZIC T. (2007) – Internal structure of the granite and tonalite intrusions in the Strzelin massif. In: Granitoids in Poland (eds. A. Kozłowski and J. Wiszniowska). AM Monograph, **1**: 217–229.

OBERC-DZIEDZIC T., KLIMAS K., KRYZA R. and FANNING C. M. (2003*a*) – SHRIMP U/Pb zircon geochronology of the Strzelin gneiss, SW Poland: evidence for a Neoproterozoic thermal event in the Fore-Sudetic Block, Central European Variscides. Int. J. Earth Sc. (Geol. Rundsch.), **92**: 701–711.

OBERC-DZIEDZIC T., KLIMAS K., KRYZA R., FANNING C. M. and MADEJ S. (2003*b*) – SHRIMP zircon ages from gneiss help locate the West-East Sudetes boundary (NE Bohemian Massif, SW Poland). J. Czech Geol. Soc. Abstr., **48** (1–2): 98.

OBERC-DZIEDZIC T., KRYZA R., KLIMAS K., FANNING M. C. and MADEJ S. (2005) – Gneiss protolith ages and tectonic boundaries in the NE part of the Bohemian Massif (Fore-Sudetic Block, SW Poland). Geol. Quart., **49** (4): 363–378.

OBERC-DZIEDZIC T. and MADEJ S. (2002) – The Variscan overthrust of the Lower Palaeozoic gneiss unit on the Cadomian basement in the Strzelin and Lipowe Hills massifs, Fore-Sudetic Block, SW Poland; is this part of the East-West Sudetes boundary? Geol. Sudet., **34**: 39–58.

OBERC-DZIEDZIC T., KRYZA R., MOCHNACKA K. and LARIONOV A. (2010) – Ordovician passive continental margin magmatism in the Central-European Variscides: U–Pb zircon data from the SE part of the Karkonosze-Izera Massif, Sudetes, SW Poland. Int. J. Earth Sc., **99**: 27–46.

OBERC-DZIEDZIC T., KRYZA R. and PIN C. (2009*a*) – The crust beneath the Polish Sudetes: evidence from a gneiss xenolith in Tertiary basanite from Paszowice. Geodinamica Acta, **22** (3): 9–31.

OBERC-DZIEDZIC T., KRYZA R. and PIN C. (2009*b*) – Granitoids as a source of knowledge of the evolution of the Earth crust in the Sudetes (SW Poland). Research Project No N307 008 32/0314, Final Report. Inst. Geol. Sc., Archiv., Wrocław.

OBERC-DZIEDZIC T. and PIN C. (2000) – The granitoids of the Lipowe Hills (Fore-Sudetic Block) and their relationship to the Strzelin granites. Geol. Sudet., **33**: 17–22.

OBERC-DZIEDZIC T., PIN C., DUTHOU J. L. and COUTURIE J. P (1996) – Age and origin of the Strzelin granitoids (Fore-Sudetic Block, Poland): $^{87}Rb/^{86}Sr$ data. N. Jb. Miner. Abh., **171**: 187–198.

OBERC-DZIEDZIC T. and SZCZEPAŃSKI J. (1995) – Geology of the Wzgórza Strzelińskie crystalline massif (in Polish with English summary). Ann. Soc. Geol. Pol. Spec. Przewodnik LXVI Zjazdu PTG: 111–126.

OLIVER G. J. H., CORFU F. and KROUGH T. E. (1993) – U/Pb ages from SW Poland: evidence for a Caledonian suture zone between Baltica and Gondwana. J. Geol. Soc., London, **150**: 355–369.

PIETRANIK A. and WAIGHT T. (2005) – Sr isotopes in plagioclase from Gęsiniec tonalite using microdrilling method (Strzelin Crystalline Massif). Miner. Soc. Pol., Spec. Pap., **26**: 231–234.

PIETRANIK A. and WAIGHT T. (2008) – Processes and sources during Late Variscan dioritic-tonalitic magmatism: insights from plagioclase chemistry (Gęsiniec Intrusion, NE Bohemian Massif, Poland). J. Petrol., **49** (9): 1619–1645.

PIN C. and SANTOS ZALDUEGUI J. F. (1997) – Sequential separation of light rare earth elements, thorium and uranium by miniaturized extraction chromatography: application to isotopic analyses of silicate rocks. Anal. Chim. Acta, **339**: 79–89.

SCHULMANN K. and GAYER R. (2000) – A model for a continental accretionary wedge developed by oblique collision: the NE Bohemian Massif. J. Geol. Soc. London, **157**: 401–416.

SCHULMANN K., KONOPÁSEK J., JANOUŠEK V., LEXA O., LARDEAUX J-M., EDEL J-B., ŠTÍPSKÁ P. and ULRICH S. (2009) – An Andean type Palaeozoic convergence in the Bohemian Massif. C. R. Geoscience, **341**: 266–286.

SKÁCEL J. (1989) – On the Lugicum-Silesicum boundary (in Czech with English summary). Acta Univ. Wratisl. 1113, Pr. Geol.-Miner., **17**: 45–55.

SŁABY E., GÖTZE J., WÖRNER G., SIMON K., WRZALIK R. and ŚMIGIELSKI M. (2008) – K-feldspar phenocrysts in microgranular magmatic enclaves: a cathodoluminescence and geochemical study of crystal growth as a marker of magma mingling dynamics. Lithos, **105**: 85–97.

STACEY J. S. and KRAMERS J. D. (1975) – Approximation of terrestrial lead isotope evolution by a two-stage model. Earth Planet. Sc. Lett., **26**: 207–221.

STEIGER R. H and JÄGER E. (1977) – Subcommission on geochronology: convention on the use of decay constants in geo- and cosmochronology. Earth Planet. Sc. Lett., **36**: 359–362.

SUESS F. E. (1912) – Die moravischen Fenster und ihre Beziehung zum Grundgebirge des Hohen Gesenke. Denkschriften der Österreichischen Akademie der Wissenschaften, Math-Nat., **88**: 541–631.

SUESS F. E. (1926) – Intrusionstektonik und Wandertektonik im variszischen Gebirge. Borntraeger Berlin.

SZCZEPAŃSKI J. (2001) – Jegłowa Beds – record of polyphase deformation in the West Sudetes contact zone (Strzelin Crystalline Massif, Fore-Sudetic Block, SW Poland (in Polish with English summary). Prz. Geol., **49** (1): 63–71.

SZCZEPAŃSKI J. (2002) – The $^{40}Ar/^{39}Ar$ cooling ages of white micas from the Jegłowa Beds (Strzelin Massif, Fore-Sudetic Block, SW Poland). Geol. Sudet., **34**: 1–7.

SZCZEPAŃSKI J. (2007) – A vestige of an Early Devonian active continental margin in the East Sudetes (SW Poland) – evidence from geochemistry of the Jegłowa Beds, Strzelin Massif. Geol. Quart., **51** (3): 271–284.

SZCZEPAŃSKI J. and JÓZEFIAK D. (1999) – Jegłowa Beds – record of polyphase deformation and metamorphism in the Strzelin crystalline massif. Mineral. Soc. Pol. Spec. Pap., **14**: 33–37.

SZCZEPAŃSKI J. and MAZUR S. (2004) – Syncollisional extension in the West/East Sudetes boundary zone (NE Bohemian Massif): structure and metamorphic record in the Jegłowa Beds from the Strzelin Massif (East Fore-Sudetic Block). N. Jb. Geol. Paläont. Abh., **233**: 297–331.

SZCZEPAŃSKI J. and OBERC-DZIEDZIC T. (1998) – Geochemistry of amphibolites from the Strzelin Crystalline Massif, Fore-Sudetic Block, SW Poland. N. Jb. Miner. Abh., **173**: 23–40.

TAYLOR S. R. and MC LENNAN S. M. (1985) – The continental crust: its composition and evolution; an examination of the geochemical record preserved in sedimentary rocks. Blackwell, Oxford.

THOMPSON R. N. (1982) – British Tertiary volcanic province. Scot. J. Geol., **18**: 49–107.

TURNIAK K., MAZUR S. and WYSOCZAŃSKI R. (2000) – SHRIMP zircon geochronology and geochemistry of the Orlica-Śnieżnik gneisses (Variscan belt of Central Europe) and their tectonic implications. Geodinamica Acta, **13**: 293–312.

TURNIAK K., TICHOMIROVA M. and BOMBACH K. (2006) – Pb-evaporation zircon ages of post-tectonic granitoids from the Strzelin Massif (SW Poland). Miner. Soc. Pol., Spec. Pap., **29**: 212–215.

Van BREEMEN O., AFTALION M., BOWES D. R., DUDEK A., MISAŘ Z., POVONDRA P. and VRANA S. (1982) – Geochronological studies of the Bohemian massif, Czechoslovakia, and their significance in the evolution of Central Europe. Trans. Royal Soc. Edinburgh: Earth Sc., **73**: 89–108.

WEDEPOHL K. H., HEINRICHS H. and BRIDGEWATER D. (1991) – Chemical characteristics and genesis of the quartz-feldspathic rocks in the Archean crust of Greenland. Contrib. Miner. Petrol., **107**: 163–179.

WIEDENBECK M., ALLÉ P., CORFU F., GRIFFIN W. L., MEIER M., OBERLI F., Von QUADT A., RODDICK J. C. and SPIEGEL W. (1995) – Three natural zircon standards for U–Th–Pb, Lu–Hf, trace element and REE analyses. Geostandards Newsletter, **19**: 1–23

WILLIAMS I. S. (1998) – U–Th–Pb Geochronology by ion microprobe. In: Applications in microanalytical techniques to understanding mineralizing processes. Rev. Econom. Geol., **7**: 1–35.

WOJNAR B. (1995) – Structural analysis and petrology of metamorphic rocks of the southern part of the Strzelin Massif (in Polish with English summary). Acta Univ. Wratisl. 1633, Pr. Geol.-Miner., **46**: 1–74.

WÓJCIK L. (1968) – Szczegółowa mapa geologiczna Sudetów. Arkusz Ciepłowody 1:25000. Inst. Geol. Wyd. Geol., Warszawa.

WROŃSKI J. (1973) – Szczegółowa mapa geologiczna Sudetów. Arkusz Ziębice 1:25 000. Inst. Geol. Wyd. Geol., Warszawa.

ZAPLETAL K. (1933) – Vznik a vývoj Tišnovska. Vlastivěda Tišnovska: 5–44. Tišnov.

ŻELAŹNIEWICZ A. and ALEKSANDROWSKI P. (2008) – Tectonic subdivision of Poland: southwestern Poland (in Polish with English summary). Prz. Geol., **56** (10): 904–911.

ŻELAŹNIEWICZ A., BUŁA Z., FANNING M., SEGHEDI A. and ŻABA J. (2009) – More evidence on Neoproterozoic terranes in Southern Poland and southeastern Romania. Geol. Quart., **53** (1): 93–124.

ŻELAŹNIEWICZ A., NOWAK I., BACHLIŃSKI R., LARIONOW A. N. and SERGEEV S. A. (2005) – Cadomian versus younger deformations in the basement of the Moravo-Silesian Variscides, East Sudetes, SW Poland: U-Pb SHRIMP and Rb-Sr age data. Geol. Sudet., **37**: 35–51.

APPENDIX

SHRIMP analytical procedure. *In situ* U-Pb analyses were performed on a SHRIMP II at the Centre of Isotopic Research (CIR) at VSEGEI (St. Petersburg), applying a secondary electron multiplier in peak-jumping mode following the procedure described in Williams (1998) and Larionov *et al*. (2004). A primary beam of molecular oxygen was employed to ablate zircon in order to sputter secondary ions. The elliptical analytical spots had a size of *ca*. 27 × 20 μm, and the corresponding ion current was *ca*. 4 nA. The sputtered secondary ions were extracted at 10 kV. The 80 μm wide slit of the secondary ion source, in combination with a 100 μm multiplier slit, allowed mass-resolution of M/ÄM >5000 (1% valley) so that all the possible isobaric interferences were resolved. One-minute rastering over a rectangular area of *ca*. 60 × 50 μm was employed before each analysis in order to remove the gold coating and possible surface common Pb contamination.

The following ion species were measured in sequence: $^{196}(Zr_2O)$-^{204}Pb-background (*ca*. 204 AMU) -^{206}Pb-^{207}Pb-^{208}Pb-^{238}U-^{248}ThO-^{254}UO with integration time ranging from 2 to 20 seconds. Four cycles for each spot analysed were acquired. Each fifth measurement was carried out on the zircon Pb/U standard TEMORA1 (Black *et al*., 2003) with an accepted ^{206}Pb/^{38}U age of 416.75 ±0.24 Ma. The 91 500 zircon with a U concentration of 81.2 ppm and a ^{206}Pb/^{238}U age of 1062.4 ±0.4 Ma (Wiedenbeck *et al*., 1995) was applied as a "U-concentration" standard. The collected results were then processed with the *SQUID v1.12* (Ludwig, 2005*a*) and *ISOPLOT/Ex 3.22* (Ludwig, 2005*b*) software, using the decay constants of Steiger and Jäger (1977). The common lead correction was done using measured ^{204}Pb according to the model of Stacey and Kramers (1975).